

Arsenate mobility through a saturated sand : effects of pore water velocity, PH and phosphate competition

by Jeffrey Edwin Darland

A thesis submitted in partial fulfillment of the requirements for the degree of Master of Science in Environmental Engineering
Montana State University
© Copyright by Jeffrey Edwin Darland (1996)

Abstract:
Previous studies have indicated that sorption of ASO4 onto soil mineral phases may be kinetically limited by diffusional processes, and other studies have demonstrated some of the effects of pH and PO4 competition on the sorption of AsO4 onto soil mineral phases. However, these studies have typically been performed in well-mixed batch systems, and it is unclear the extent to which data derived from batch experiments may be extrapolated to a transport condition. Consequently, the objective of this study was to determine the effects of pore water velocity, pH, and PO4 competition on the transport of AsO4 through a model sand where the principle reactive phase was amorphous or poorly crystalline Fe-oxides. The convection-dispersion equation (CDE) was used to predict the saturated transport of AsO4 through the sand at four different pore water velocities (PWVs) using equilibrium and kinetic expressions to describe the sorption of AsO4 by the sand. Saturated column transport experiments were performed using an applied AsO4 pulse (133 pM) through a disturbed sand at PWVs of 0.2, 1.0, 10, and 90 cm h^-1 (pH=4.5). In addition, saturated transport studies were performed in the presence of 0, 13.4, 134, and 1340 pM PO4, at pH values of 4.5, 6.5, and 8.5 (PWV=1 cm h^-1).

Observed AsO4 breakthrough curves (BTCs) demonstrated sorption related nonequilibrium at pH=4.5 at all PWVs. The use of independently derived equilibrium and kinetic sorption parameters (batch) in the CDE failed to describe observed BTCs at all PWVs. Fitting of kinetic rate parameters in the CDE to the observed BTCs resulted in different apparent sorption rate parameters at each PWV modeled. Enhanced mobility of AsO4 at pH=8.5 was identified as a pH effect. PO4 competition resulted in increased AsO4 mobility, however even in the presence of excess PO4 significant amounts of AsO4 remained sorbed to the sand. The indication is that AsO4 desorption kinetics play an important role in transport of AsO4 through porous media. Furthermore, sorption rates of AsO4 during transport appear to be highly dependent upon PWV, suggesting that kinetic data obtained from batch studies may not be extrapolatable to all transport conditions.

ARSENATE MOBILITY THROUGH A SATURATED SAND: EFFECTS OF PORE WATER VELOCITY, pH AND PHOSPHATE COMPETITION

by

Jeffrey Edwin Darland

A thesis submitted in partial fulfillment
of the requirements for the degree

of

Master of Science

in

Environmental Engineering

MONTANA STATE UNIVERSITY
Bozeman, Montana

January 1996

© COPYRIGHT

by

Jeffrey Edwin Darland

1996

All Rights Reserved

N378
D2489

APPROVAL

of a thesis submitted by

Jeffrey Edwin Darland

This thesis has been read by each member of the thesis committee and has been found to be satisfactory regarding content, English usage, format, citations, bibliographic style, and consistency, and is ready for submission to the College of Graduate Studies.

Jan 16, 1996
Date

Chairperson, Graduate Committee

Approved for the Major Department

1/16/96
Date

Head, Major Department

Approved for the College of Graduate Studies

2/10/96
Date

Graduate Dean

STATEMENT OF PERMISSION TO USE

In presenting this thesis in partial fulfillment of the requirements for a master's degree at Montana State University, I agree that the Library shall make it available to borrowers under rules of the Library.

If I have indicated my intention to copyright this thesis by including a copyright notice page, copying is allowable only for scholarly purposes, consistent with "fair use" as prescribed in the U.S. Copyright Law. Requests for permission for extended quotation from or reproduction of this thesis in whole or in parts may be granted only by the copyright holder.

Signature Jeffrey E Hurlbut/ORS

Date Jan 16, 1996

ACKNOWLEDGMENTS

I would not have been able to complete this work without the support of others. I would like to thank Dr. William Inskeep, Dr. Hesham Gaber, and Dr. Jon Wraith for their help and support in this work. I would also like to thank Dr. Otto Stein, without whose support I never would have made it out to Montana State University, and Dr. Warren Jones for serving as a member of my graduate committee.

I would also like to thank Clain Jones, Heiko Langner, Dr. Shaobai Sun, and Rich Macur, who were forced to share both a lab and their knowledge.

Finally, I would like to thank my parents, Paula Larson and Lawrence Stein, and my wife, Colette, for all of the love and support given to me during this endeavor.

TABLE OF CONTENTS

LIST OF TABLES vii

LIST OF FIGURES viii

ABSTRACT x

1. INTRODUCTION 1

2. EFFECTS OF PORE WATER VELOCITY ON THE TRANSPORT OF AsO_4 THROUGH A SAND 3

2.1. Introduction 4

2.2. Transport Model Formulations 6
2.2.1. Equilibrium Partitioning Models 8
2.2.2. Non-Equilibrium Partitioning Models 8

2.3. Materials and Methods 10
2.3.1. Reagents and Analysis 10
2.3.2. Kinetic Adsorption Study 11
2.3.3. Batch Isotherms 12
2.3.4. Column Transport Experiments 12
2.3.5. Determination of Column Transport Parameters 13

2.4. Results 14
2.4.1. Kinetic Adsorption Study 14
2.4.2. Batch Adsorption Isotherms 15
2.4.3. Determination of Kinetic Adsorption/Desorption Rate Parameters 15
2.4.4. Column Transport Experiments 17
2.4.5. Predicted Breakthrough Curves - LEA 20
2.4.6. Predicted Breakthrough Curves - Kinetic Reversible Sorption 22
2.4.7. Fitted Breakthrough Curves - nth-order kinetic 24

2.5. Discussion 27

2.6. Conclusions 29

2.7. Nomenclature 31

TABLE OF CONTENTS - Continued

3. EFFECTS OF pH AND PHOSPHATE COMPETITION ON THE TRANSPORT OF AsO_4 THROUGH A SAND 32

3.1. Introduction 33

3.2. Materials and Methods 35
3.2.1. Reagents and Analysis 35
3.2.2. Kinetic Adsorption Study 36
3.2.3. Batch Isotherms 37
3.2.4. Column Transport Experiments 37
3.2.5. Determination of Column Transport Parameters 40

3.3. Results and Discussion 41
3.3.1. Batch Adsorption 41
3.3.2. Effects of pH on As Transport 44
3.3.3. Effects of Phosphate Competition on As Transport 50

3.4. Conclusions 55

4. CONCLUSIONS AND GENERAL DISCUSSION 56

4.1. Implications for Modeling 58

4.2. Implications for Soil Liming 62

4.3. Implications for PO_4 Application 62

5. REFERENCES 64

LIST OF TABLES

Table 1: Sorbed phase accumulation terms used in the basic convection-dispersion equation (CDE)..... 7

Table 2: Physical and chemical characteristics of sand used. Surface area determined by triple point BET N_2 isotherms. Total chemical composition determined by Li-metaborate fusion. "Free" Al and Fe determined by citrate-dithionite (C-D) extraction. Numbers in parentheses indicate standard deviation of three samples. 10

LIST OF FIGURES

Figure 1: Adsorption kinetics of AsO_4 onto sand and FITMRM model results for first- and nth-order kinetic models. Experimental conditions: 1:1 solid:solution ratio (5 g (dry weight) solid:5 mL solution); pH range = 4 to 5; 150 μM initial AsO_4 in a background solution of 0.01 M KCl..... 14

Figure 2: Adsorption isotherms (Background: 0.01 M KCl) for AsO_4 at a 1:2 solid:solution ratio (5 g (dry weight) solid:10 mL solution) and a pH range of 4.0 to 4.6. Fitted lines represent (i) the linear isotherm using an approximate K_D of 200 L kg^{-1} to fit the linear portion of the data, and (ii) the Freundlich isotherm where K_F and 1/n were fit using nonlinear regression..... 16

Figure 3: Observed and predicted (CXTFIT) ^3H_2O breakthrough curves at three different pore water velocities (1, 10, and 90 cm h^{-1}). Column conditions: Background = 0.01 M KCl; ^3H_2O pulse = 1 pore volume..... 18

Figure 4: Observed AsO_4 breakthrough curves to 10 pore volumes, at four different pore water velocities (PWVs) (0.2, 1, 10, and 90 cm h^{-1}). Column conditions: Background = 0.01 M KCl; AsO_4 pulse = 1 pore volume at 133 μM. 19

Figure 5: Predicted (MRTM) AsO_4 distribution in sand columns after 50 pore volumes total flow under the LEA using independent estimates of linear (——) and Freundlich (- - -) adsorption parameters and dispersion coefficients from ^3H_2O BTCs (column conditions: background = 0.01 M KCl; AsO_4 pulse = 1 pore volume at 133 μM): (a) pore water concentration; (b) sorbed phase concentration 21

Figure 6: Observed (×) and predicted AsO_4 BTCs (MRTM) for first (- - -) and nth-order (——) kinetic adsorption expressions at three different pore water velocities (PWVs) using kinetic parameters derived from batch experiments (column conditions: background = 0.01 M KCl; AsO_4 pulse = 1 pore volume at 133 μM): (a) PWV=1 cm h^{-1}; (b) PWV=10 cm h^{-1}; (c) PWV=90 cm h^{-1}..... 23

Figure 7: Observed (×) and fitted (——) AsO_4 breakthrough curves (BTCs) obtained by optimizing rate parameters (k_f, k_r, n) of the nth-order kinetic adsorption expression at three different pore water velocities (PWVs). Predicted (- - -) AsO_4 BTCs are shown for 10 and 90 cm h^{-1} PWV treatments using fitted rate parameters determined at 1 cm h^{-1} (column conditions: background = 0.01 M KCl; AsO_4 pulse = 1 pore volume at 133 μM): (a) PWV=1 cm h^{-1}; (b) PWV=10 cm h^{-1}; (c) PWV=90 cm h^{-1}..... 26

LIST OF FIGURES - Continued

Figure 8: Adsorption kinetics of AsO_4 and PO_4 onto sand (single ion experiment) at a 1:1 solid:solution ratio (5 g (dry weight) solid:5 mL solution and at pH values ranging from 4 to 5 (AsO_4) and 4 to 5.7 (PO_4)). Initial concentrations were 150 μM AsO_4 and 360 μM PO_4 in a background solution of 0.01 M KCl. 42

Figure 9: Adsorption isotherms (0.01 M KCl) for AsO_4 in the absence and presence of 134 μM and 1340 μM PO_4 at a 1:1 solid:solution ratio (15 g (dry weight) solid:15 mL solution) and a pH range of 4.0 to 4.6. Solid lines represent best fit Langmuir isotherms, where Γ_0 = maximum adsorption density and K_L = empirical affinity parameter. 43

Figure 10: The transport of AsO_4 through a sand at three different carbonate buffered pH values: 4.5, 6.5 and 8.5 (Column conditions: Pore water velocity = 1 cm h^{-1}; Background = 0.01 M KCl; AsO_4 pulse = 1 pore volume at 133 μM)..... 45

Figure 11: The transport of AsO_4 through clean quartz sand (Fluka) at pH 7 (Column conditions: Pore water velocity = 1 cm h^{-1}; Background = 0.01 M KCl; AsO_4 pulse = 1 pore volume at 133 μM). 46

Figure 12: The distribution of AsO_4 species (solid lines represent concentration, dashed lines represent activity) as a function of pH for conditions specific to the column experiments (0.01 M KCl, 133 μM AsO_4); based on: pK_{a1}=2.24, pK_{a2}=6.94, pK_{a3}=11.5 (Sadiq et al., 1983). 48

Figure 13: The transport of AsO_4 through sand at pH 8.5 in the presence and absence of CO_2(g) buffering (Column conditions: Pore water velocity = 1 cm h^{-1}; Background = 0.01 M KCl; AsO_4 pulse = 1 pore volume at 133 μM). 49

Figure 14: The transport of AsO_4 through sand at pH 4.5 in the presence of 0, 13.4, 134, and 1340 μM PO_4 (Column conditions: Pore water velocity = 1 cm h^{-1}; Background = 0.01 M KCl; AsO_4 pulse = 1 pore volume at 133 μM). 50

Figure 15: The transport of AsO_4 through sand at pH 6.5 (CO_2(g) buffered) in the presence of 0, 13.4, 134, and 1340 μM PO_4 (Column conditions: Pore water velocity = 1 cm h^{-1}; Background = 0.01 M KCl; AsO_4 pulse = 1 pore volume at 133 μM). 51

Figure 16: The transport of AsO_4 through sand at pH 4.5 followed by continuous addition of 1420 μM PO_4 at ~20 pore volumes (Column conditions: Pore water velocity = 1 cm h^{-1}; Background = 0.01 M KCl; AsO_4 pulse = 1 pore volume at 143 μM). 53

ABSTRACT

Previous studies have indicated that sorption of AsO_4 onto soil mineral phases may be kinetically limited by diffusional processes, and other studies have demonstrated some of the effects of pH and PO_4 competition on the sorption of AsO_4 onto soil mineral phases. However, these studies have typically been performed in well-mixed batch systems, and it is unclear the extent to which data derived from batch experiments may be extrapolated to a transport condition. Consequently, the objective of this study was to determine the effects of pore water velocity, pH, and PO_4 competition on the transport of AsO_4 through a model sand where the principle reactive phase was amorphous or poorly crystalline Fe-oxides. The convection-dispersion equation (CDE) was used to predict the saturated transport of AsO_4 through the sand at four different pore water velocities (PWVs) using equilibrium and kinetic expressions to describe the sorption of AsO_4 by the sand. Saturated column transport experiments were performed using an applied AsO_4 pulse (133 μM) through a disturbed sand at PWVs of 0.2, 1.0, 10, and 90 cm h^{-1} (pH=4.5). In addition, saturated transport studies were performed in the presence of 0, 13.4, 134, and 1340 μM PO_4, at pH values of 4.5, 6.5, and 8.5 (PWV=1 cm h^{-1}). Observed AsO_4 breakthrough curves (BTCs) demonstrated sorption related nonequilibrium at pH=4.5 at all PWVs. The use of independently derived equilibrium and kinetic sorption parameters (batch) in the CDE failed to describe observed BTCs at all PWVs. Fitting of kinetic rate parameters in the CDE to the observed BTCs resulted in different apparent sorption rate parameters at each PWV modeled. Enhanced mobility of AsO_4 at pH=8.5 was identified as a pH effect. PO_4 competition resulted in increased AsO_4 mobility, however even in the presence of excess PO_4 significant amounts of AsO_4 remained sorbed to the sand. The indication is that AsO_4 desorption kinetics play an important role in transport of AsO_4 through porous media. Furthermore, sorption rates of AsO_4 during transport appear to be highly dependent upon PWV, suggesting that kinetic data obtained from batch studies may not be extrapolatable to all transport conditions.

1. INTRODUCTION

Arsenic (As) is an important contaminant in many reclamation sites containing fly ash and mining waste, and exists in elevated concentration in soils impacted by natural and geothermal sources (e.g., Madison River Valley, Montana) (Sonderegger and Ohguchi, 1988) as well. Since As presents a significant health hazard in groundwaters used for domestic purposes, there is a need to understand processes affecting As transport in soils, sediments, and aquifers, especially in regions where groundwater is a principle source of domestic drinking water.

There has been substantial previous research on processes affecting As (as AsO_4) sorption by soils and soil mineral phases. Such research has included kinetic studies of adsorption onto oxide mineral phases (e.g. Grossl, 1995; Fuller et al., 1993), the effects of pH on sorption (e.g. Anderson, et al., 1976; Pierce and Moore, 1982; Goldberg, 1986; Hingston et al., 1971), and the effects of anion competition with phosphate (PO_4) during sorption (e.g. Hingston et al., 1971; Goldberg, 1986; Peryea, 1991); and these processes have been successfully quantified and modeled in batch systems. It is unclear, however, the extent to which batch derived data (typically involving well-mixed low solid:solution ratios) may be extrapolated to transport environments, particularly as regards coupling these processes with existing transport models.

This thesis comprises two studies designed to elucidate factors affecting As transport (as AsO_4) through saturated soils and aquifers. In particular, Chapter 2

investigates the effect of pore water velocity and subsequent kinetic limitations that can occur during AsO_4 transport. The role of soil water pH and PO_4 competition on the transport of AsO_4 is investigated in Chapter 3. The objectives of the current studies were to determine:

(i) the applicability of batch derived equilibrium and kinetic partitioning parameters in transport models describing AsO_4 transport through a representative sand,

(ii) the effects of pore water velocity on sorption rate coefficients derived during AsO_4 transport,

(iii) the effect of pH on AsO_4 transport,

(iv) the extent to which simultaneous competition between AsO_4 and PO_4 for adsorption sites affects AsO_4 transport,

(v) the effect of pH on the competition between AsO_4 and PO_4 for adsorption sites during transport, and

(vi) the extent to which modification of pore water PO_4 concentration could increase AsO_4 mobility in contaminated aquifer sands.

2. EFFECTS OF PORE WATER VELOCITY ON THE TRANSPORT OF AsO_4 THROUGH A SAND

Previous studies have shown that the sorption of AsO_4 by Fe- and Al-oxide minerals may be kinetically limited by diffusional processes even under well-mixed batch conditions. The potential for AsO_4 to exhibit sorption related nonequilibrium during transport has not been previously determined. Consequently, the objectives of this study were to determine the applicability of transport models based on the convection-dispersion equation (CDE) using equilibrium (linear and Freundlich) and kinetic (first- and nth-order) sorption expressions in describing AsO_4 mobility. Saturated column transport experiments were performed using an applied AsO_4 pulse (1 pore volume, 133 μM $^{73}AsO_4$) at pore water velocities (PWVs) of 0.2, 1.0, 10, and 90 cm h^{-1} through a sand where the principle reactive phase was amorphous or poorly crystalline Fe-oxides. Observed AsO_4 breakthrough curves (BTCs) exhibited poor recovery and significant tailing at all pore water velocities, and demonstrated sorption related nonequilibrium as evidenced by a leftward shift in observed BTCs and an increase in observed effluent recovery with increasing PWV. The use of independently derived equilibrium and kinetic sorption parameters (batch) and column dispersion coefficients (from ^3H_2O BTCs) in the CDE failed to describe observed AsO_4 BTCs at all pore water velocities. Rate parameters obtained by fitting observed BTCs to the nth-order kinetic model resulted in different apparent sorption rate coefficients and isotherm nonlinearity parameters as a function of PWV. Fitted apparent adsorption and desorption rate coefficients increased with increasing PWV. The results of this study indicate that sorption rates of AsO_4 onto soils and aquifer materials during transport are highly dependent upon pore water velocity, and that kinetic data obtained from batch studies cannot be readily extrapolated to all transport conditions.

2.1. Introduction

The two principle forms of As in groundwaters are AsO_3 (As(III)) and AsO_4 (As(V)). Under oxidizing environments where AsO_4 is generally predominant relative to AsO_3, and solution concentrations of AsO_4 do not exceed the solubility product of metal arsenate solid phases, soluble equilibrium AsO_4 concentrations can be expected to be controlled by adsorption onto mineral surfaces. Moreover, AsO_4 is generally preferentially sorbed to metal oxide surfaces compared to layer silicates (Fordam and Norrish, 1979; Jacobs et al., 1970; Johnson and Barnard, 1979; Livesey and Huang, 1981; Fuller et al., 1993). Arsenate adsorption by Fe hydroxides can be categorized as a ligand exchange mechanism, and it has been shown by Extended X-ray Absorption Fine Structure Spectroscopy (EXAFS) that AsO_4 forms a combination of mono- and bidentate complexes with surface Fe sites (Waychunas et al., 1993). For AsO_4 adsorption onto α-FeOOH, these ligand exchange reactions have been represented by (Goldberg, 1986; Grossl, 1995):

$$FeOH(s) + H_3AsO_4(aq) = FeH_2AsO_4(s) + H_2O$$
$$FeOH(s) + H_3AsO_4(aq) = FeHAsO_4^-(s) + H_2O + H^+(aq)$$
$$FeOH(s) + H_3AsO_4(aq) = FeAsO_4^{2-}(s) + H_2O + 2H^+(aq)$$
$$2FeOH(s) + H_3AsO_4(aq) = Fe_2HAsO_4(s) + 2H_2O$$
$$2FeOH(s) + H_3AsO_4(aq) = Fe_2AsO_4^-(s) + 2H_2O + H^+(aq)$$

and have successfully described equilibrium sorption conditions over the pH range of 3.5 to 10 using the Constant Capacitance model.

The actual chemical step describing the surface complexation of AsO_4 onto Fe oxides and clay minerals is quite rapid, generally on the order of milliseconds (Grossl, 1995; Amacher, 1991; Sparks and Zhang, 1991). Studies have shown, however, that even in well-mixed batch systems the approach to equilibrium can be slow, on the order of hours, for AsO_4 adsorption onto amorphous Al-hydroxides (Anderson et al., 1976) and ferrihydrite (Fuller et al., 1993). These results indicate that mass transfer limitations such as interparticle, intraparticle, and film diffusion may play a significant role in the kinetics of AsO_4 sorption onto soil minerals phases (Fuller et al., 1993). The extent to which these kinetic processes may affect the transport of AsO_4 through soils and/or aquifer materials is unclear.

Sorption processes influenced by slow mass transfer rates may be subject to chemical (sorption related) nonequilibrium under transport conditions (Brusseau, 1992). Under these situations, it is characteristic to observe changes in the shape (e.g. tailing) of solute breakthrough curves as a function of pore water velocity (Bouchard et al., 1988; Brusseau, 1992; Gaber et al., 1992; Gaber et al., 1995). Moreover, transport derived rate constants representing the adsorption/desorption process may vary with pore water velocity (Gaber et al., 1995; Brusseau, 1992; Gamerdinger et al., 1991), indicating that the diffusional processes controlling adsorption/desorption rates are sensitive to the mixing environment (Ball et al., 1991).

While there has been substantial research on batch equilibrium sorption reactions of AsO_4 onto geological minerals and natural soils, there have been few studies investigating the role of kinetic limitations on AsO_4 sorption by soils. Furthermore, there

is a lack of detailed data on the effects of kinetic processes on AsO_4 transport through porous media. The primary goal of the current study was to elucidate the adsorption effects and kinetic limitations on AsO_4 transport through a saturated sand. In particular, the objectives were to (i) determine the applicability of two equilibrium adsorption models (linear and Freundlich) and two simple kinetic adsorption models (first-order and nth-order reversible) in describing AsO_4 transport using the convection-dispersion equation (CDE), and (ii) to determine the effect of pore water velocity on apparent sorption rate coefficients derived during As transport.

2.2. Transport Model Formulations

The convection-dispersion equation (CDE) describes the one-dimensional steady-state transport of adsorbing solutes through soils:

$$\rho \frac{\delta s}{\delta t} + \theta \frac{\delta c}{\delta t} = \theta \cdot D \frac{\delta^2 c}{\delta x^2} - v \frac{\delta c}{\delta x} \qquad (1)$$

where ρ represents soil bulk density [$M\ L^{-3}$], s represents sorbed concentration [$M\ M^{-1}$], t represents time [T], θ represents volumetric water content [$L^3\ L^{-3}$], c represents solute concentration [$M\ L^{-3}$], D represents the hydrodynamic dispersion coefficient [$L^2\ T^{-1}$], v represents average pore water velocity [$L\ T^{-1}$], and x represents distance [L]. The left side of this mass-balance equation represents the accumulation of solute in the sorbed ($\delta s/\delta t$) and liquid ($\delta c/\delta t$) phases, while the right side represents mass flux of solute due to dispersion and convection.

Travis and Etnier (1981) provided a fairly comprehensive review of the relationships used to quantify adsorption of reactive solutes by soils. Fundamentally, the

adsorption of solutes can be modeled as either an equilibrium or a kinetic process, depending on whether or not the sorbed phase is locally at equilibrium with the resident solution phase concentration. Common equilibrium and kinetic expressions used to describe the change in sorbed phase concentration ($\delta s/\delta t$) in the CDE are presented in Table 1, corresponding to adsorption described by both the linear and the Freundlich isotherms, where K_D, K_F, K_D', and K_F' are distribution coefficients [$L^3\ M^{-1}$], k_f is a forward reaction rate constant [T^{-1}], k_r is a reverse reaction rate constant [T^{-1}], and n is a dimensionless Freundlich reaction order.

Table 1: Sorbed phase accumulation terms used in the basic convection-dispersion equation (CDE).

	Model	Sorbed Phase Accumulation Term	Partitioning at Equilibrium
Case A.	Linear Equilibrium	$\frac{\delta s}{\delta t} = K_D \cdot \frac{\delta c}{\delta t}$	$s = K_D \cdot c$
Case B.	Freundlich Equilibrium	$\frac{\delta s}{\delta t} = \frac{K_F}{n} c^{(1/n - 1)} \cdot \frac{\delta c}{\delta t}$	$s = K_F \cdot c^{1/n}$
Case C.	First-Order Reversible	$\frac{\delta s}{\delta t} = \frac{\theta}{\rho} k_f c - k_r s$	$s = K_D' \cdot c$ $K_D' = \frac{\theta}{\rho} \frac{k_f}{k_r}$
Case D.	nth-Order Reversible	$\frac{\delta s}{\delta t} = \frac{\theta}{\rho} k_f c^{1/n} - k_r s$	$s = K_F' \cdot c^{1/n}$ $K_F' = \frac{\theta}{\rho} \frac{k_f}{k_r}$

2.2.1. Equilibrium Partitioning Models

It is often assumed that the resident solution phase concentration is locally at equilibrium with the sorbed phase concentration (defined as the Local Equilibrium Assumption, LEA). Solutions to the CDE using the LEA have employed the linear isotherm (e.g., Lapidus and Amundson, 1952) (Table 1, Case A) and the Freundlich isotherm (Sidle et al., 1977, Bahr and Rubin, 1987; Selim et al., 1990) (Table 1, Case B). One of the principle benefits of these expressions is that the adsorbed solute concentration can be described solely as a function of soluble concentration, which greatly simplifies the numerically integrated solution of the CDE. There have been many published reports, however, which indicate that nonequilibrium conditions during transport preclude the use of the LEA with either linear or Freundlich isotherms (Valocchi, 1985; Parker and Valocchi, 1986; Bahr and Rubin, 1987; Gaber et al., 1992).

2.2.2. Non-Equilibrium Partitioning Models

Transport models based on the CDE using kinetic expressions to describe adsorption processes have also been previously published (van Genuchten et al., 1974; Sparks and Jardine, 1984; Bahr and Rubin 1987; Selim et al., 1990). The simplest kinetic expression is a first-order reversible reaction (Table 1, Case C), which at equilibrium corresponds to a linear isotherm (Sparks and Jardine, 1984; Bahr and Rubin 1987). Kinetic expressions describing nth-order reversible adsorption (which at equilibrium reduces to the Freundlich isotherm) have also been used in the CDE (Table 1, Case D) (e.g. van Genuchten et al., 1974; Bahr and Rubin, 1987; Selim et al., 1990). Additional

approaches for modeling nonequilibrium conditions during the transport of reactive solutes include defining different sorption domains. For example, the two site nonequilibrium model (Cameron and Klute, 1977; Parker and van Genuchten, 1984; Brusseau et al., 1991) assumes instantaneous sorption in one domain and rate limited sorption in another domain (rate limited sorption described by the first-order reversible reaction). Selim et al. (1990) considered the soil system as a complex combination of up to five different types of reaction sites (domains) including equilibrium reversible Freundlich, kinetic nth-order reversible, and kinetic nth-order irreversible adsorption.

If any transport model is to be used in a predictive role, a certain number of input parameters must be obtained independently from external sources. Common sources of this information include laboratory batch studies or tabulated literature values. Generally, the number of required input parameters increases with model complexity. In a practical sense, minimization of the complexity of the input requirements is desired. While previous work has been directed toward assessing the applicability of particular models, most of this previous work is directed toward the applicability of the LEA (e.g. Valocchi, 1985; Parker and Valocchi, 1986; Bahr and Rubin, 1987; Gaber et al., 1992) and the existing literature has focused primarily on the transport of organic or heavy metal contaminants. Few studies have been directed toward the applicability of these models to the transport of AsO_4, which is an important contaminant in soils, aquifers, and surface waters. Moreover, the extent to which batch derived equilibrium and/or kinetic parameters may be useful for predicting AsO_4 transport is unclear.

2.3. Materials and Methods

2.3.1. Reagents and Analysis

Sand of mixed mineralogy was obtained from the Unimin Corporation, Emmett, Idaho (Granusil Grade 50), sieved to a particle size range of 0.25 to 0.50 mm, acid washed with 0.05 M HCl (3 times), then rinsed with double deionized water (DD-H_2O) until the conductivity of the rinse stabilized at <2μS. The sand was then oven dried at 105°C, and characterized for surface area (SA), cation exchange capacity (CEC), amorphous Fe and Al hydroxides by citrate-dithionite extraction (Olson and Ellis, 1982), and chemical composition by total dissolution (Table 2).

Table 2: Physical and chemical characteristics of sand used. Surface area determined by triple point BET N_2 isotherms. Total chemical composition determined by Li-metaborate fusion. "Free" Al and Fe determined by citrate-dithionite (C-D) extraction. Numbers in parentheses indicate standard deviation of three samples.

Element	%-by weight	Deviation
Si	36.798	(0.454)
K	4.044	(0.414)
Al	3.764	(0.251)
Ca	0.570	(0.035)
Na	0.311	(0.086)
Fe	0.054	(0.025)
Mn	<0.002	
P	<0.002	
Fe-"Free"	0.010	(0.001)
Al-"Free"	<0.010	

Particle Size: 0.25 to 0.50 mm - seived
Surface Area: 0.390 ± 0.034 m^2/g
CEC: 2.7×10^{-3} mmol charge/g

All AsO_4 solutions were prepared with the same source of analytical grade Na_2HAsO_4 salt (Baker), and diluted with DD-H_2O. Solution AsO_4 concentrations were measured by three different methods depending on the experiments performed. For batch studies, AsO_4 was measured by atomic absorption with continuous hydride generation (AA-HG). For transport studies, radiolabeled $^{73}AsO_4$ (Los Alamos National Laboratory) was used in conjunction with liquid scintillation (LS). Ion chromatography (IC) was used (Dionex AS4A-SC) periodically to verify concentrations determined by LS, and to verify that no reduction of AsO_4 to AsO_3 had occurred during the experiments. The purity of the AsO_4 stock solutions was verified by IC.

2.3.2. Kinetic Adsorption Study

A batch study was performed to determine the adsorption kinetics of AsO_4 onto the sand, and to determine an equilibrium time required for batch adsorption isotherm experiments. The kinetic adsorption experiments were performed in 15-mL polyethylene screw top bottles (Nalgene), and consisted of a 1:1 solid to solution ratio (5 g solid:5 mL solution), using initial concentrations of 150 μM AsO_4. All solutions were prepared in a background of 0.01 M KCl. Samples were collected at time intervals of 2, 4, 8, 24, 48, 96, and 168 h, and were decanted and filtered through 0.45μ nylon filters prior to analysis by AA-HG. Adsorbed concentrations were then determined by difference between initial and final measured solute concentrations.

2.3.3. Batch Isotherms

Batch adsorption isotherms for AsO_4 onto the sand were performed in duplicate in 35-mL polypropylene centrifuge tubes (Nalgene), and were performed using a 1:2 solid to solution ratio (5 g solid:10 mL solution). Initial concentrations of 1.33, 4.00, 13.3, 40.0, 133, 400, and 667 μM AsO_4 were used, in a background of 0.01 M KCl. Samples were shaken for 168 h, then decanted and filtered through 0.45μ nylon filters prior to analysis by AA-HG. Adsorbed concentrations were determined by difference between initial and final measured solute concentrations.

2.3.4. Column Transport Experiments

Column transport experiments were performed using 2.8-cm inside diameter, 8-cm length polycarbonate columns containing ~76.5 g sand, resulting in a bulk density of ~1.55 g cm^{-3} and a calculated porosity of ~0.41. The end caps of the columns consisted of fine nylon mesh (<0.1 mm) supported by a Teflon plate drilled with 1-mm holes on 3-mm centers. A syringe pump (Soil Measurement Systems, Tucson, AZ) was used to deliver eluant to the bottom of each column. Four different pore water velocities were established in separate column runs (0.2, 1.0, 10, and 90 cm h^{-1}) using intermittent syringe pump pulses. After initial saturation and conditioning with 0.01 M KCl, approximately 1 pore volume of a tritiated water solution (^3H_2O in 0.01 M KCl background, ~500 Bq mL^{-1}) was pulsed through the columns as a conservative tracer, followed by an eluant of 0.01 M KCl. After complete recovery of the ^3H_2O pulse (~6 pore volumes total flow), one pore volume of 133 μM ^{73}As-labeled AsO_4 (~1650 Bq mL^{-1}, 0.01 M KCl background) was applied followed by 0.01 M KCl. The experiments were continued until the tailing of AsO_4 in

column effluent was well established (~20 pore volumes), and AsO_4 concentrations approached baseline levels.

Column effluent was passed through an in-line 0.45μ nylon filter and collected in glass test tubes using a fraction collector (~8 samples per pore volume). Effluent samples were analyzed for pH, followed by ^{73}As activity as determined by LS. Periodic determinations of AsO_4 concentration by IC verified that no reduction of AsO_4 had occurred during transport. After termination, the sand from the columns was extracted with a mixture of 6N HCl and 3N HNO_3 to desorb the remaining sorbed AsO_4, and the resulting extract analyzed for ^{73}As activity using LS to verify complete recovery of all applied As. In all cases, the total recovery of applied As was greater than 95%.

2.3.5. Determination of Column Transport Parameters

The volumes of column effluent samples were determined by mass, and the water flux (q) determined as the average sample volume divided by the collection interval. Pore water velocity (v) was then determined as $q\,\theta^{-1}$ where θ was calculated using the relation $\theta = 1-(\rho/2.65)$, assuming a particle density of 2.65 g cm^{-3} and complete saturation in the columns. Breakthrough curves (BTCs) for ^3H_2O were fitted to the one-dimensional CDE with the computer program CXTFIT (Parker and van Genuchten, 1984) assuming no adsorption of ^3H_2O (retardation factor = 1) to determine column dispersion coefficients (D). All ^3H_2O BTCs were symmetrical, exhibited no tailing, and conformed to the CDE based on the LEA with r^2 values > 0.99. These criteria were used to verify a lack of

transport related (physical) nonequilibrium in the column transport experiments (Brusseau, 1992).

2.4. Results

2.4.1. Kinetic Adsorption Study

The kinetics of AsO_4 adsorption onto sand showed that approximately 97% of the equilibrium adsorbed AsO_4 concentration was reached within 24 h (Figure 1). Equilibrium (as defined by constancy of the ratio of adsorbed AsO_4 concentration to aqueous AsO_4

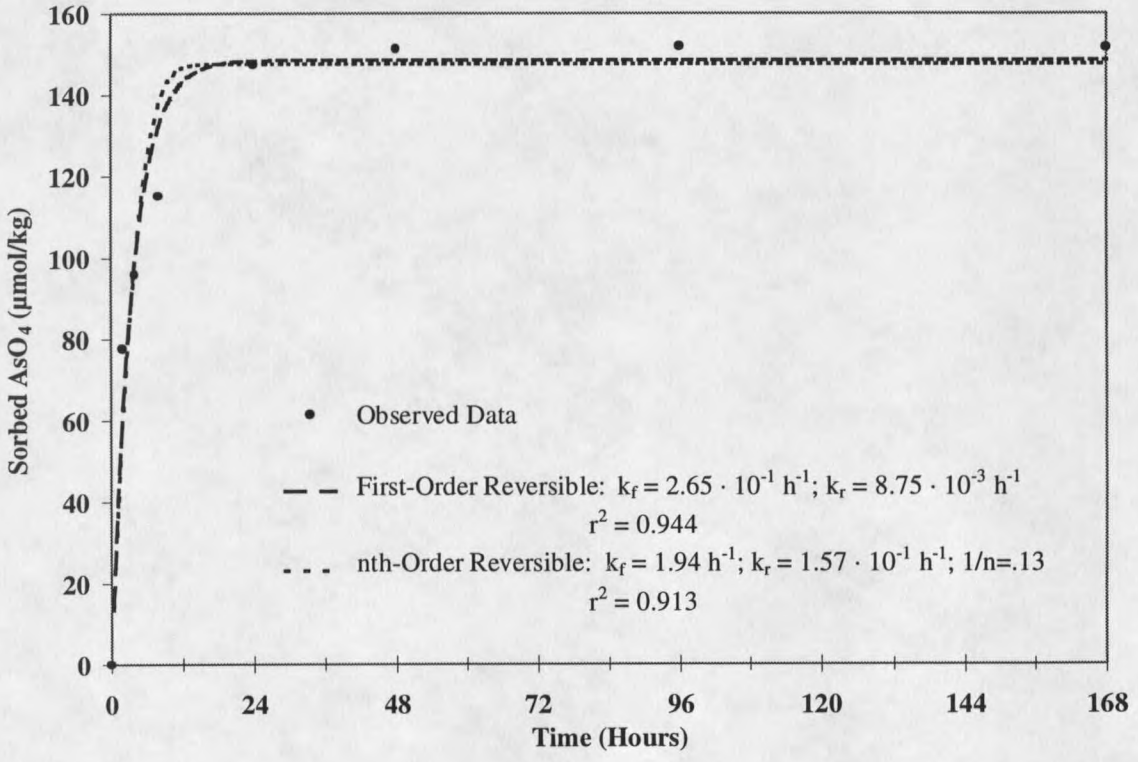


Figure 1: Adsorption kinetics of AsO_4 onto sand and FITMRM model results for first- and nth-order kinetic models. Experimental conditions: 1:1 solid:solution ratio (5 g (dry weight) solid:5 mL solution); pH range = 4 to 5; 150 µM initial AsO_4 in a background solution of 0.01 M KCl.

concentration) was not reached until at least 96 h, which is consistent with other studies showing a slow approach to equilibrium for AsO_4 sorption onto amorphous Al hydroxides (Anderson et al., 1976) and ferrihydrite (Fuller et al., 1993). Since the actual chemical step for the adsorption reaction of AsO_4 onto Fe and Al oxides and clay mineral surfaces has been shown to occur on the order of milliseconds (Grossl, 1995; Amacher et al., 1991; Sparks and Zhang, 1991), the slower approach to equilibrium observed in this experiment suggests that the kinetics of AsO_4 adsorption onto the sand were likely limited by intra or interaggregate diffusional processes.

2.4.2. Batch Adsorption Isotherms

The sorption of AsO_4 onto the sand showed nonlinear behavior above equilibrium solution concentrations of 10 μM AsO_4 (Figure 2). At low As concentrations (< 10 μM AsO_4), the adsorption data was approximately linear; in this range the adsorption data could be described by the linear isotherm (Table 1, Case A), using a K_D = ~200 L kg^{-1}. The complete set of observed adsorption data were modeled to the best fit (nonlinear regression) Freundlich isotherm (Table 1, Case B), resulting in a K_F = 24.6 L kg^{-1} and 1/n=0.13 (r^2=0.961).

2.4.3. Determination of Kinetic Adsorption/Desorption Rate Parameters

In order to determine an independent estimate of kinetic adsorption/desorption rate parameters for use in predictive transport models, the batch kinetic adsorption data (Figure 1) were fit to the first-order reversible and the nth-order reversible adsorption models (Table 1, Cases C and D, respectively) using the computer program FITMRM

(Selim et al., 1990), assuming the presence of a single kinetically limited phase in the sand. For the first-order reversible model, both the forward and reverse rate constants (k_f and k_r, respectively) were allowed to vary independently, resulting in $k_f = 2.65 \times 10^{-1}$ h^{-1} and $k_r = 8.75 \times 10^{-3}$ h^{-1} (r^2=0.944). The fitted rate constants yield an apparent equilibrium linear distribution coefficient ($K_D' = \frac{\theta}{\rho} \frac{k_f}{k_r}$) at a 1:1 solid:solution ratio of ~30 L kg^{-1}, as compared with the approximated K_D = 200 L kg^{-1} (Figure 2).

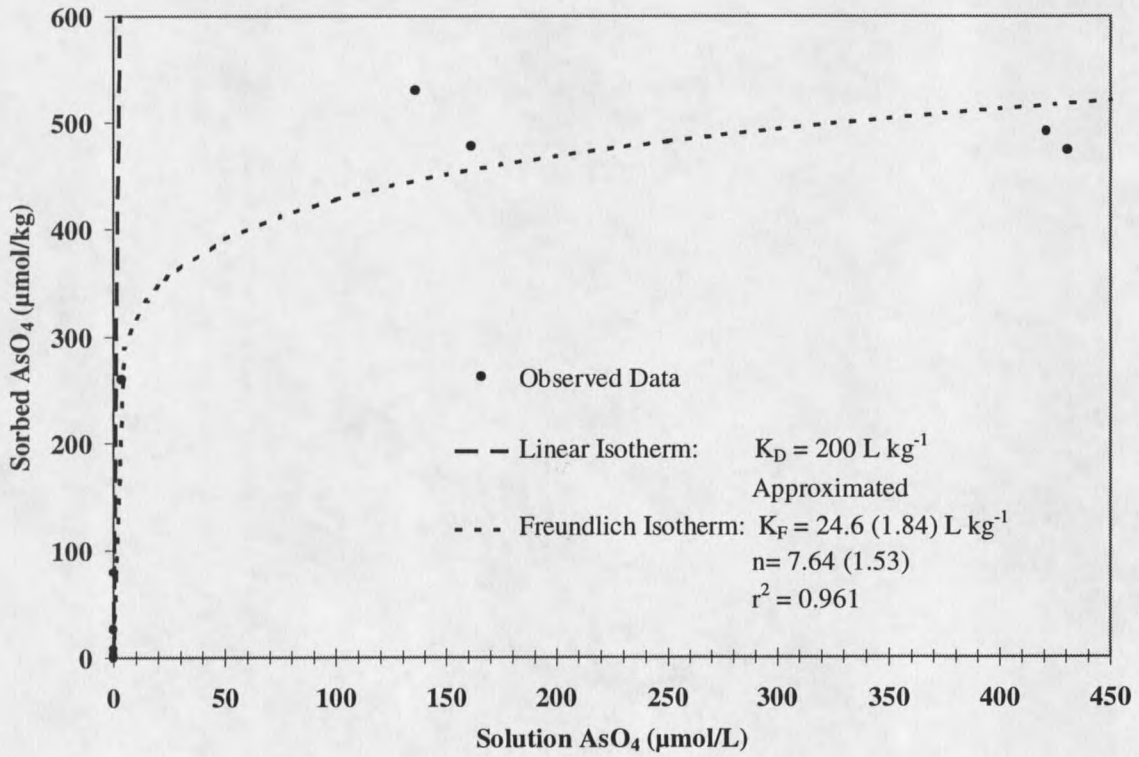


Figure 2: Adsorption isotherms (Background: 0.01 M KCl) for AsO_4 at a 1:2 solid:solution ratio (5 g (dry weight) solid:10 mL solution) and a pH range of 4.0 to 4.6. Fitted lines represent (i) the linear isotherm using an approximate K_D of 200 L kg^{-1} to fit the linear portion of the data, and (ii) the Freundlich isotherm where K_F and n were fit using nonlinear regression. Standard errors are presented in parentheses for fit data.

Forward and reverse rate constants (k_f and k_r, respectively) corresponding to the nth-order reversible reaction (Table 1, Case D) were determined by fixing the ratio of k_f/k_r and the reaction order such that the apparent Freundlich equilibrium distribution coefficient ($K_F' = \frac{\theta}{\rho}\frac{k_f}{k_r}$) and the dimensionless Freundlich reaction order (n) were equal to values as determined from batch equilibrium isotherms (K_F = 24.6 L kg^{-1}, 1/n = 0.13). Nonlinear regression fits resulted in k_f = 1.94 h^{-1} and $k_r = 1.57 \times 10^{-1}$ h^{-1} (r^2 = 0.913).

2.4.4. Column Transport Experiments

Column dispersion coefficients were determined from ^3H_2O BTCs using CXTFIT (Parker and van Genuchten, 1984), at pore water velocities of 1 cm h^{-1} (D=0.1058 cm^2 h^{-1}, r^2=0.999), 10 cm h^{-1} (D=0.8305 cm^2 h^{-1}, r^2=0.991), and 90 cm h^{-1} (D=16.31 cm^2 h^{-1}, r^2=0.998), and indicated that no transport related nonequilibrium occurred in the column experiments (Figure 3). ^3H_2O was not used in the slowest pore water velocity (0.2 cm h^{-1}), consequently, no dispersion coefficient was determined for that column experiment. Additional saturated column transport experiments performed in related experiments (Chapter 3) using the same columns and sand under the same packing conditions have all indicated that transport related (physical) nonequilibrium was not important over this range in pore water velocities. The column transport experiments were performed using unbuffered pulse and eluant solutions. Pore water pH, as determined by measurement of effluent samples, fell within the pH range of 4.0 to 4.5 for all transport experiments.

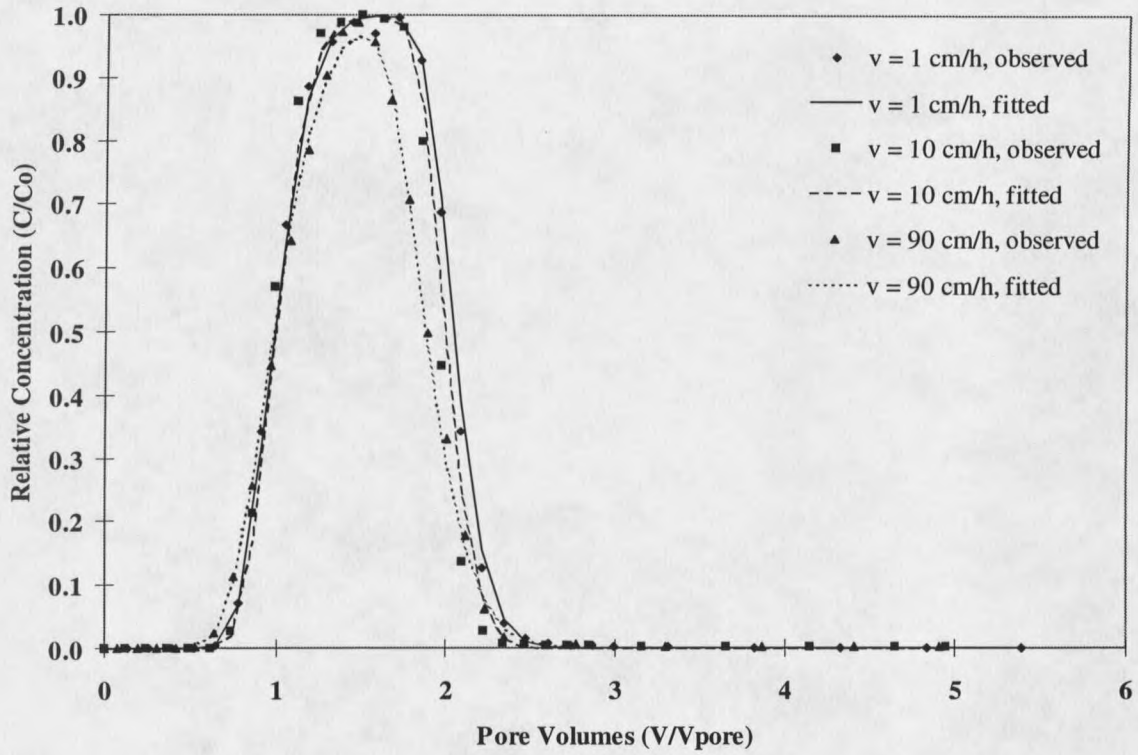


Figure 3: Observed and predicted (CXTFIT) ^3H_2O breakthrough curves at three different pore water velocities (1, 10, and 90 cm h^{-1}). Column conditions: Background = 0.01 M KCl; ^3H_2O pulse = 1 pore volume.

Breakthrough curves (BTCs) showing the effect of pore water velocity on AsO_4 transport through the sand are presented in Figure 4. Significant breakthrough and tailing of AsO_4 was evidenced in all but the slowest pore water velocity treatments (0.2 cm h^{-1}). Arsenic BTCs exhibited a leftward shift and increased recovery of applied AsO_4 in the column effluent with increasing pore water velocity. The percent of applied AsO_4 recovered in the column effluent after 10 pore volumes total flow was 7.24, 35.6, 53.3, and 74.3 % for columns at pore water velocities of 0.2, 1, 10, and 90 cm h^{-1}, respectively. The increased recovery of AsO_4 in column effluent and the leftward shift in the BTCs with increasing pore water velocity is consistent with sorption related nonequilibrium, and

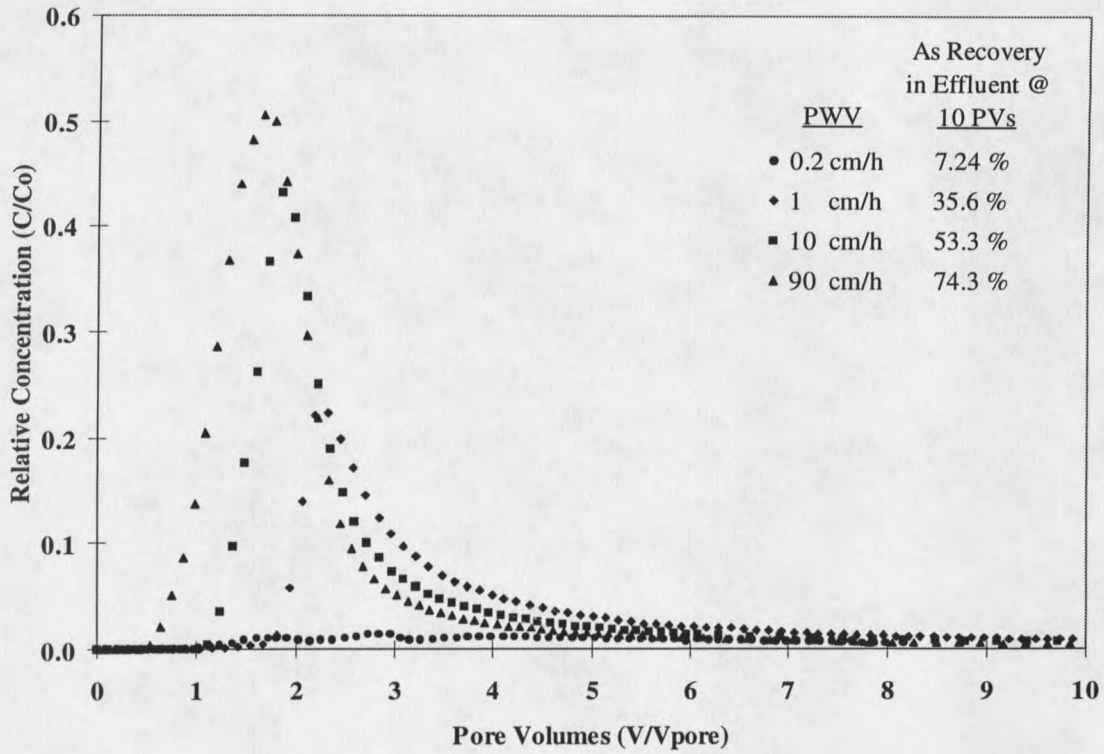


Figure 4: Observed AsO_4 breakthrough curves to 10 pore volumes, at four different pore water velocities (PWVs) (0.2, 1, 10, and 90 cm h^{-1}). Column conditions: Background = 0.01 M KCl; AsO_4 pulse = 1 pore volume at 133 μM.

indicates that at pore water velocities of 1 cm h^{-1} or greater adsorption equilibrium was not reached during transport. Since no transport experiments were performed at pore water velocities slower than 0.2 cm h^{-1}, it is unclear whether sorption related nonequilibrium existed at a pore water velocity of 0.2 cm h^{-1}. However, as will be discussed in a subsequent section, the recovery of even 7% AsO_4 at 0.2 cm h^{-1} would not be expected based on local equilibrium assumptions.

2.4.5. Predicted Breakthrough Curves - LEA

The CDE (based on the LEA) was used to predict the transport of AsO_4 for both the linear and the Freundlich adsorption isotherm expressions using the computer program MRTM (Selim et al., 1990), using independent estimates of AsO_4 adsorption parameters obtained from batch isotherm experiments (K_D = 200 L kg^{-1}; K_F = 24.62 L kg^{-1}, 1/n = 0.13) and dispersion coefficients calculated from ^3H_2O BTCs using CXTFIT (Parker and van Genuchten, 1984). No breakthrough of AsO_4 was predicted at any pore water velocity within 20 pore volumes total flow under the LEA for either the linear or the Freundlich adsorption models. Predicted transport data for As generated using MRTM for both linear and Freundlich sorption (PWV = 1 cm h^{-1}) were obtained up to 50 pore volumes. The leading edge of the predicted AsO_4 BTC had progressed less than 2 cm through an 8 cm column (Figure 5). In contrast, observed AsO_4 BTCs in column effluent occurred within 2 pore volumes total flow at all pore water velocities (Figure 4). In addition, measured As concentrations from post-run dissected columns at all pore water velocities indicated a relatively uniform distribution of As throughout the column after only 20 pore volumes total flow. Finally, the fact that 7% of applied AsO_4 was recovered in column effluent at 0.2 cm h^{-1} suggests that sorption related nonequilibrium existed even at this relatively slow pore water velocity (< 5 cm d^{-1}).

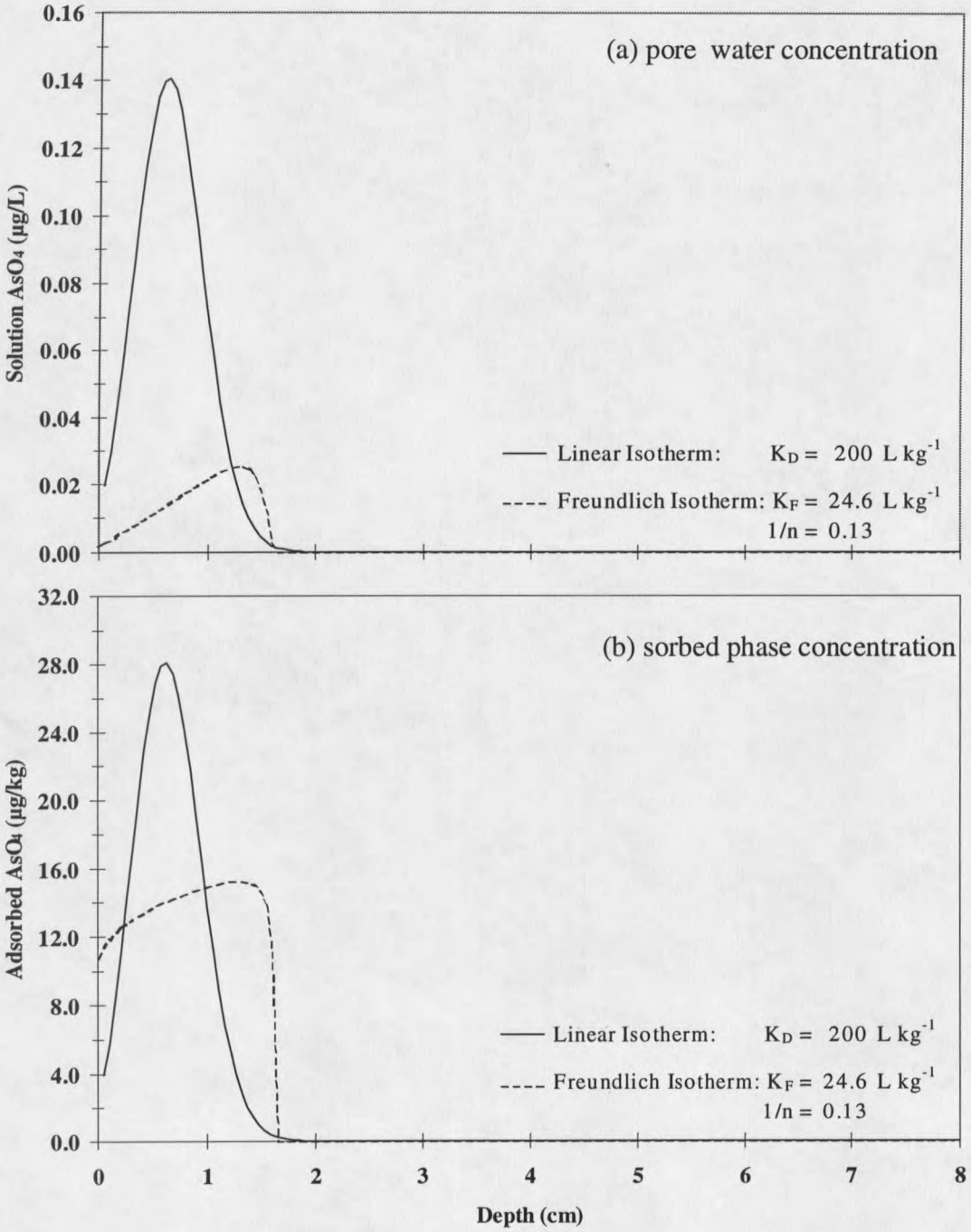


Figure 5: Predicted (MRTM) AsO_4 distribution in sand columns after 50 pore volumes total flow under the LEA using independent estimates of linear (——) and Freundlich (- - -) adsorption parameters and dispersion coefficients from ^3H_2O BTCs (column conditions: background = 0.01 M KCl; AsO_4 pulse = 1 pore volume at 133 µM): (a) pore water concentration; (b) sorbed phase concentration

2.4.6. Predicted Breakthrough Curves - Kinetic Reversible Sorption

Fitted batch kinetic sorption parameters for the first-order reversible reaction were used along with PWVs (measured) and dispersion coefficients (^3H_2O BTCs) to predict (MRTM) the transport of AsO_4 at pore water velocities of 1, 10, and 90 cm h^{-1} (Figure 6). Predicted recoveries of AsO_4 in column effluent for the first-order reversible sorption model at 10 pore volumes total flow were 28.1, 81.9, and 96.4 % at PWVs of 1, 10, and 90 cm h^{-1}, respectively. Although predicted AsO_4 BTCs based on a first-order reversible kinetic model were closer to observed data than predictions based on the LEA, the first-order kinetic model uniformly failed to describe the significant tailing observed in column experiments. The failure of the first-order reversible sorption model to adequately describe the transport of AsO_4 was not surprising considering that batch equilibrium isotherms of AsO_4 onto sand were nonlinear (Figure 2). The first-order kinetic parameters determined from batch experiments correspond at equilibrium to an apparent linear distribution coefficient (K_D') of ~ 30 L kg^{-1}, which failed to describe equilibrium sorption at low (<100 μM) and high (>200 μM) AsO_4 solution concentrations.

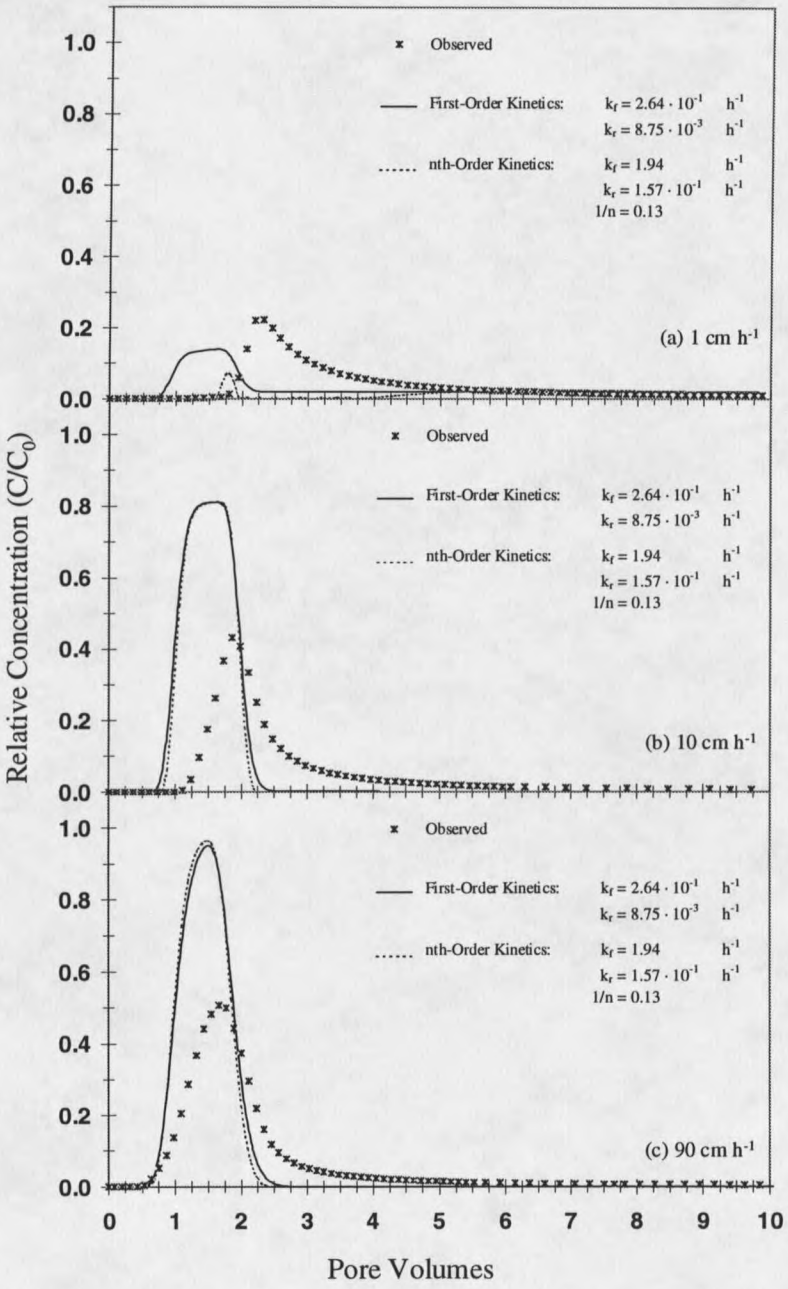


Figure 6: Observed (×) and predicted AsO_4 BTCs (MRTM) for first (- - -) and nth-order (——) kinetic adsorption expressions at three different pore water velocities (PWVs) using kinetic parameters derived from batch experiments (column conditions: background = 0.01 M KCl; AsO_4 pulse = 1 pore volume at 133 µM): (a) PWV=1 cm h^{-1}; (b) PWV=10 cm h^{-1}; (c) PWV=90 cm h^{-1}.

Arsenic BTCs were also predicted (MRTM) from the nth-order reversible kinetic model using column dispersion coefficients (^3H_2O) and batch derived kinetic parameters (Figure 6). At 10 pore volumes total flow, predicted AsO_4 recoveries in column effluent were 13.0, 76.1, and 96.9 % at PWVs of 1, 10, and 90 cm h^{-1}, respectively. Similar to the first-order reversible kinetic model, the observed tailing was greater than that predicted by the nth-order kinetic model. Predicted BTCs for the nth- and first-order kinetic models were essentially identical at pore water velocities of 10 and 90 cm h^{-1}. In both kinetic models, predicted BTCs were more symmetrical and resulted in greater As recovery compared to observed data. Predicted breakthrough curves occurred at ~ 1 pore volume with peak heights ranging from 0.8 to 0.95 (C/C_0). Peak heights of observed BTCs did not exceed 0.5, indicating that both the first- and nth-order kinetic models underestimated AsO_4 sorption (or overestimated AsO_4 desorption) at PWVs of 10 and 90 cm h^{-1}.

2.4.7. Fitted Breakthrough Curves - nth-order kinetic

The nth-order reversible kinetic model (Table 1, Case D) was fit to the observed AsO_4 BTCs at a pore water velocity of 1 cm h^{-1} using the computer program FITMRTM (Selim et al., 1990), by varying the rate coefficients for adsorption and desorption (k_f and k_r) and the reaction order (n). Optimized model parameters at 1 cm h^{-1} were $k_f = 7.31$ h^{-1}, $k_r = 8.21 \times 10^{-1}$ h^{-1}, and $1/n = 9.27 \times 10^{-2}$ ($r^2 = 0.990$) (Figure 7(a)). The transport determined rate coefficients and the reaction order (n) were greater than those determined by batch ($k_f = 1.94$ h^{-1}, $k_r = 1.57 \times 10^{-1}$ h^{-1}, $1/n = 0.13$; Figure 1). The rate parameters (k_f, k_r, n) obtained from fitting the experimental data at 1 cm h^{-1} PWV were then used to predict the transport of AsO_4 under column conditions at 10 cm h^{-1} and 90 cm h^{-1}.

Predicted AsO_4 BTCs based on 1 cm h^{-1} rate parameters did not accurately represent AsO_4 transport at 10 and 90 cm h^{-1} (Figure 7(b) and 7(c)). The fact that predicted BTCs overestimated As transport at 10 and 90 cm h^{-1} suggests that sorption rate coefficients determined at 1 cm h^{-1} were too slow to describe the processes occurring at the higher PWV treatments.

Least squares curve fitting (MRTM) of the observed AsO_4 BTCs under column conditions at 10 cm h^{-1} and 90 cm h^{-1} was also performed (varying k_f, k_r, and 1/n), yielding at 10 cm h^{-1}: $k_f = 22.98\ h^{-1}$, $k_r = 3.58\ h^{-1}$, and 1/n = 0.13 ($r^2 = 0.942$), and at 90 cm h^{-1}: $k_f = 66.22\ h^{-1}$, $k_r = 33.24\ h^{-1}$, and 1/n = 0.40 ($r^2 = 0.954$). Comparison of fitted AsO_4 BTCs at 10 and 90 cm h^{-1} demonstrates improved description of AsO_4 transport behavior when the rate coefficients of the nth-order model vary with PWV.

In summary, fitted (optimized) nth-order rate coefficients were highly affected by (i) the method of determination (batch vs. column), and (ii) variations in column PWV. The rate coefficients (k_f and k_r) determined by batch were slower than those determined by column, and the column determined rate coefficients increased with increasing PWV. The apparent $K_F' \left(\frac{\theta}{\rho}\frac{k_f}{k_r}\right)$ determined by batch was 46.7 L kg^{-1}, compared with K_F' values of 33.6, 24.2, and 7.56 L kg^{-1} determined from column experiments at PWVs of 1, 10, and 90 cm h^{-1}, respectively. The apparent degree of nonlinearity of the fitted nth-order kinetic sorption model (1/n) also varied with changes in the pore water velocity. The batch 1/n value was 0.13, compared with 1/n values of 0.093, 0.13, and 0.40 determined from column experiments at PWVs of 1, 10, and 90 cm h^{-1}, respectively.

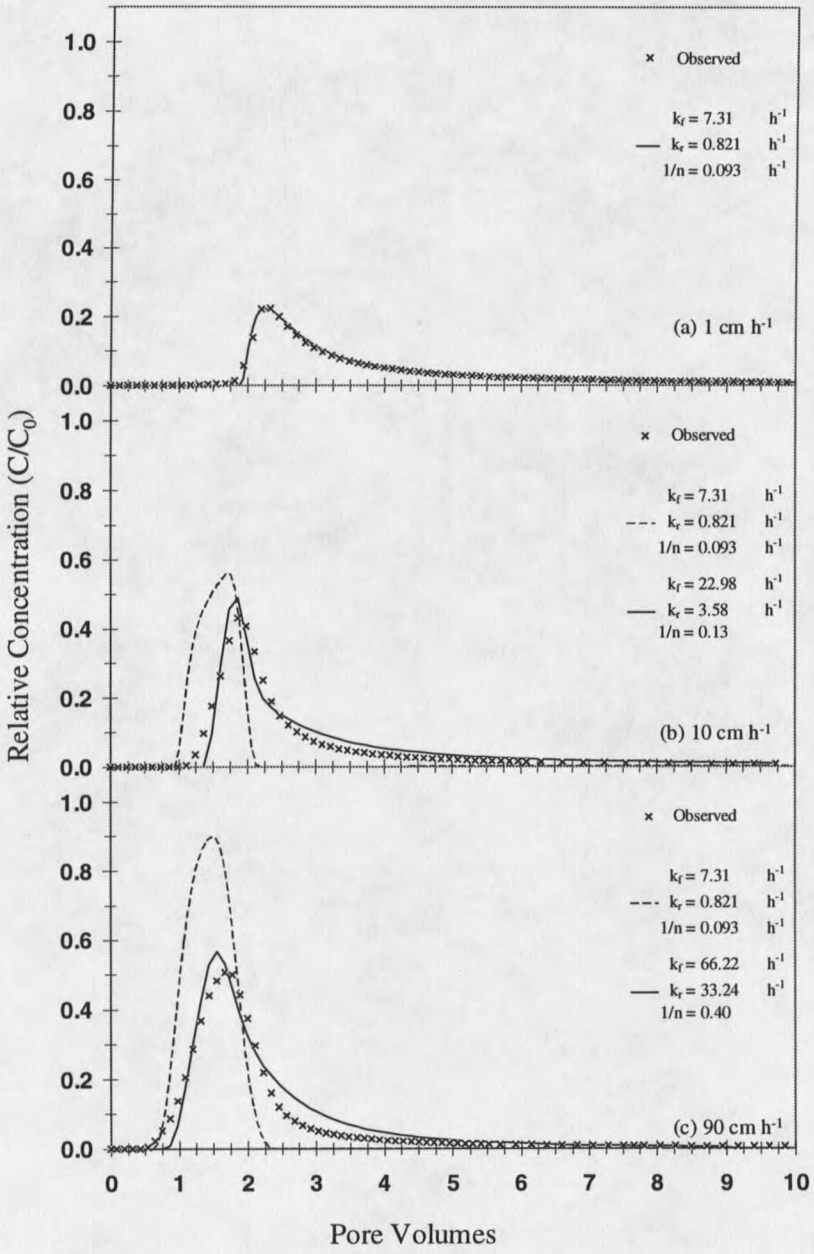


Figure 7: Observed (×) and fitted (——) AsO_4 breakthrough curves (BTCs) obtained by optimizing rate parameters (k_f, k_r, n) of the nth-order kinetic adsorption expression at three different pore water velocities (PWVs). Predicted (- - -) AsO_4 BTCs are shown for 10 and 90 cm h^{-1} PWV treatments using fitted rate parameters determined at 1 cm h^{-1} (column conditions: background = 0.01 M KCl; AsO_4 pulse = 1 pore volume at 133 μM): (a) PWV=1 cm h^{-1}; (b) PWV=10 cm h^{-1}; (c) PWV=90 cm h^{-1}.

2.5. Discussion

Hydrodynamic dispersion is typically considered to be the predominant, if not only, source of dispersion observed in disturbed column transport studies with uniformly packed, nonaggregated soils. In actuality, observed dispersion is a combination of hydrodynamic dispersion and axial, film, and intraparticle diffusion. It has been demonstrated by Brusseau (1993) that in a typical sandy soil hydrodynamic dispersion accounted for >95% of all dispersion, with contributions from axial diffusion (<5%), film diffusion (<0.001%), and intraparticle diffusion (<0.1%) being small to nonexistent. Transport related nonequilibrium (TNE) is typically attributed to large heterogeneities in pore-scale water velocities (Parker and van Genuchten, 1984), which are usually caused by relatively stagnant regions within aggregated particles or by preferential flow pathways. In the current study, observed BTCs of a nonreacting tracer (^3H_2O) verified the absence of significant transport related nonequilibrium (Figure 3), which is consistent with the findings of Brusseau (1993). Consequently, the observed nonequilibrium in the current study was not considered to be a result of TNE (as described in the bicontinuum TNE models presented by Parker and van Genuchten (1984) and Brusseau et al. (1991)) but rather due to kinetic processes specific to AsO_4.

The actual chemical step of AsO_4 adsorption onto reactive soil mineral phases is quite rapid (Grossl, 1995; Amacher, 1991; Sparks and Zhang, 1991). Consequently, in the absence of diffusion limitations (inter or intraparticle), rate coefficients describing the actual chemical steps in the sorption process should be independent of column transport conditions. It is clear from the current study that significant variation in sorption rate

coefficients was observed as a function of column PWV. Consequently, it appears that processes other than single site chemical adsorption are controlling the kinetic partitioning of AsO_4 under the transport conditions of this experiment.

In a related study, Chapter 3 suggests that Fe-oxyhydroxides were the principle reactive phases in the sand used in this study, even though the overall "Free" Fe content in the sand was less than 0.1% by weight (Table 2). Previous investigators have suggested that surface precipitation of ferric arsenates may occur on ferrihydrite at high AsO_4 concentrations (Pierce and Moore, 1982). In more recent work by Waychunas et al. (1993), however, EXAFS spectroscopy showed no evidence of As-bearing surface precipitates or solid solutions in AsO_4/ferrihydrite systems at total AsO_4 concentration of 5 mM, which is more than an order of magnitude higher than the AsO_4 pulse concentrations used in this study. Also, ion activity products (IAPs) for Fe and Al arsenates under conditions present in the column and batch experiments (assuming Fe and Al levels in equilibrium with amorphous oxide minerals) did not exceed the solubility limits for known arsenate solid phases. Consequently, it is expected that surface precipitation did not affect the kinetic sorption rates observed in this study.

Fuller et al. (1993) have demonstrated that diffusional processes may be extremely important in controlling adsorption and desorption rates of AsO_4 on surface coordination sites on ferrihydrite. If this is indeed the case, then observed sorption rate coefficients will be highly dependent upon mixing rates and flow characteristics resulting from transport processes, and will not necessarily be constant over a range of pore water velocities. Furthermore, rate coefficients determined from batch experiments would not necessarily

be applicable to transport environments with substantially different flow and mixing rates. This is consistent with the opinions presented by Ball et al. (1991) that a priori prediction of diffusionally limited sorption rates is not possible.

2.6. Conclusions

Transport of AsO_4 through a sand exhibited chemical (sorption related) nonequilibrium behavior over a wide range of pore water velocities (0.2 to 90 cm h^{-1}) as determined by observed breakthrough curves (BTCs) and the uniform failure of the convection-dispersion equation (CDE) using the local equilibrium assumption (LEA) to accurately predict transport using either linear or Freundlich adsorption models. Attempts to predict AsO_4 BTCs with a first-order reversible sorption rate expression using independent rate coefficients determined from batch kinetic experiments were not successful in describing AsO_4 transport. Predicted AsO_4 BTCs generated with an nth-order kinetic expression using independent rate parameters determined from batch kinetic experiments also failed to accurately predict observed BTCs at all modeled pore water velocities.

Curve fitting the observed AsO_4 BTCs using the nth-order kinetic model resulted in different apparent adsorption/desorption rate coefficients (k_f, k_r) and a different degree of nonlinearity (1/n) at each pore water velocity modeled. Increases in PWV resulted in increases in the fitted adsorption and desorption rate coefficients (k_f and k_r), a decrease in the apparent equilibrium distribution coefficient K_F', and an increase in the nonlinearity term of the reaction model (1/n). The variation of fitted rate coefficients with changes in column PWV suggests that sorption rates are affected by diffusional processes. This is

consistent with results of Fuller et al. (1993) showing that diffusional processes may be extremely important in controlling sorption rates of AsO_4 onto ferrihydrite in batch experiments. Data from the current study show that sorption rates of AsO_4 onto Fe-oxyhydroxide surfaces during transport through a model sand are greatly affected by pore water velocity. Consequently rate coefficients determined from well mixed batch studies or from any given column PWV cannot be readily extrapolated to all transport conditions.

2.7. Nomenclature

c = soluble concentration [$M\ L^{-3}$]

s = solid phase adsorbed concentration [$M\ M^{-1}$]

v = average pore water velocity [$L\ T^{-1}$]

t = time [T]

ρ = bulk density [$M\ L^{-3}$]

θ = volumetric water content [$L^3\ L^{-3}$]

D = hydrodynamic dispersion coefficient [$L^2\ T^{-1}$]

R = dimensionless retardation factor

K_D = linear distribution coefficient [$L^3\ M^{-1}$]

K_F = Freundlich distribution coefficient [$L^3\ M^{-1}$]

n = dimensionless Freundlich reaction order

α = reaction rate constant [T^{-1}]

k_f = forward reaction rate constant [T^{-1}]

k_r = backward reaction rate constant [T^{-1}]

F = fraction of instantaneous sites

K_D' = apparent equilibrium linear distribution coefficient [$L^3\ M^{-1}$]

K_F' = apparent equilibrium Freundlich distribution coefficient [$L^3\ M^{-1}$]

3. EFFECTS OF pH AND PHOSPHATE COMPETITION ON THE TRANSPORT OF AsO_4 THROUGH A SAND

There is significant interest in understanding soil chemical processes which may influence the fate and transport of AsO_4 in natural systems. The effects of pH and PO_4 competition on AsO_4 sorption by soils and aquifer materials have been previously investigated in batch studies; however such studies are typically well-mixed at high solution:solid ratios and may not be universally applicable to transport conditions. Consequently, the objective of this study was to determine the effects of pH and PO_4 on AsO_4 sorption under transport conditions where reaction and mass transfer rates may be controlling pore water AsO_4 concentrations. Saturated column transport experiments were performed using a model sand (pore water velocity = 1 cm h^{-1}) in which a one pore volume pulse of $^{73}AsO_4$ (133 μM) was applied in the presence of 0, 13.4, 134, and 1340 μM PO_4 at pH values of 4.5, 6.5, and 8.5. An additional transport experiment (pH=4.5) was performed in which a column was contaminated with an AsO_4 pulse (1 pore volume, 143 μM) and eluted for 20 pore volumes after which a constant pulse of PO_4 (1420 μM) was applied to the column. The maximum sorption site density for AsO_4 on the sand was determined using batch conditions to be 168 μmol kg^{-1}, with amorphous Fe-oxides comprising the principle reactive solid phase. AsO_4 breakthrough curves exhibited poor recovery and significant tailing at pH values of 4.5 and 6.5 in the absence of PO_4. A substantial increase in AsO_4 mobility at pH 8.5 was identified as a pH effect and not a result of HCO_3^-/CO_3^{2-} competition. PO_4 competition resulted in increased AsO_4 mobility, however, even in the presence of PO_4 levels representing more than 100% of maximum sorption capacity for the columns, significant amounts of AsO_4 remained sorbed to the sand. The application of a continuous PO_4 pulse to a column containing sorbed AsO_4 resulted in an increase in AsO_4 recovery of more than 35%; however, even after total PO_4 loading exceeded the column capacity by more than two orders of magnitude, approximately 40% of the applied AsO_4 remained sorbed to the sand. These results indicate that rates of AsO_4 desorption play an important role in transport of AsO_4 through porous media.

3.1. Introduction

The pH dependence of arsenate (AsO_4) adsorption has been investigated on numerous solid phases including amorphous Al hydroxide (Anderson et al., 1976), amorphous Fe hydroxide (Pierce and Moore, 1982), goethite and gibbsite (Goldberg, 1986; Hingston et al., 1971), kaolinite, montmorillonite, calcite, and quartz (Goldberg and Glaubig, 1988; Frost and Griffin, 1977; Xu et al., 1991). It is well established that adsorption of AsO_4 on Fe and Al hydroxides (including goethite and gibbsite) increases with decreasing pH to pH values near 3. Arsenate sorption on calcite and layer silicate minerals generally shows a maximum in the pH range of 4 to 6. Adsorption of AsO_4 onto clean, crystalline quartz was demonstrated to be negligible at pH values above 3 (Xu et al., 1991). The existing adsorption data show that in natural systems, AsO_4 is preferentially adsorbed to Fe and Al oxide minerals compared to kaolinite, montmorillonite, calcite or quartz (Fordam and Norrish, 1979; Jacobs et al. 1970; Johnston and Barnard, 1979; Livesey and Huang, 1981).

Research has also shown substantial competition between AsO_4 and phosphate (PO_4) sorption on a variety of soils and oxide minerals (Goldberg, 1986; Hingston et al., 1971; Peryea, 1991; Roy et al., 1986a; Roy et al., 1986b). In soils that have been previously contaminated with lead AsO_4 pesticides, application of PO_4 fertilizers has been shown to result in increased As mobility (Peryea, 1991). Hingston et al. (1971) modeled the competition between AsO_4 and PO_4 on both goethite and gibbsite by a modified Langmuir isotherm using selectivity coefficients derived from experimental data involving binary mixtures over a wide range of concentrations. This approach has been extended to

natural soils as well (Roy et al., 1986a; Roy et al., 1986b). Goldberg (1986) successfully used a constant capacitance model to predict the competition between AsO_4 and PO_4 on gibbsite over a range of AsO_4 and PO_4 solution concentrations, with surface complexation constants determined from a binary system in which AsO_4 and PO_4 were present in equimolar amounts.

While there has been substantial research on the effects of pH and PO_4 competition on AsO_4 adsorption in batch studies, there is little data regarding the effects of these processes on transport of AsO_4 through porous media. Furthermore, while these processes have been quantified and modeled in batch systems, such systems typically are well-mixed with high solution to solid ratios, and represent near equilibrium conditions. It is unclear the extent to which such data may be extrapolated to transport environments where reaction and mass transfer rates may be controlling pore water AsO_4 concentrations (Chapter 2). Consequently, the objectives of this research were to determine (i) the effect of pH on AsO_4 transport through a representative sand, (ii) the extent to which simultaneous competition between AsO_4 and PO_4 for adsorption sites affects AsO_4 transport in a typical sand, (iii) the effect of pH on the competition between PO_4 and AsO_4 for adsorption sites during transport, and (iv) the extent to which modification of pore water PO_4 concentration could increase AsO_4 mobility in contaminated aquifer sands. The focus of this study was to elucidate processes important in the transport of As under oxidizing conditions where As(V) is the predominant species. Appropriate mathematical expressions necessary for modeling the transport of As under column conditions are discussed in a separate study (Chapter 2).

3.2. Materials and Methods

3.2.1. Reagents and Analysis

Sand of mixed mineralogy was obtained from the Unimin Corporation (Emmett, Idaho), sieved to a particle size range of 0.25 to 0.50 mm, acid washed with 0.05 N HCl (3X), then rinsed with double deionized water (DD-H_2O) until the conductivity of the rinse had stabilized at < 2 μS. The sand was then oven dried at 105°C, and characterized for surface area and chemical composition (Table 1). In addition, an acid purified quartz sand (SiO_2) was obtained (Fluka) pre-sieved to a particle size distribution of 0.074 mm to 0.42 mm and used in selected AsO_4 transport experiments. All chemical impurities in the purified quartz sand were below detection, as given by the manufacturer.

All AsO_4 solutions were prepared with the same source of analytical grade Na_2HAsO_4 salt (Baker), and diluted with DD-H_2O. Arsenate concentrations were measured by three different methods depending on the experiments performed. For the batch studies, AsO_4 was measured by atomic absorption with continuous hydride generation (AA-HG). For the transport studies, radiolabeled $^{73}AsO_4$ (Los Alamos National Laboratory) was used in conjunction with liquid scintillation counting. Ion chromatography (IC) was used (Dionex AS4A-SC column) periodically to verify concentrations determined by liquid scintillation, and to verify that no reduction of arsenate to arsenite had occurred.

All PO_4 solutions were prepared with the same source of analytical grade K_2HPO_4 salt (Baker), and diluted with DD-H_2O. Phosphate concentrations were measured by two

different methods depending on the experiments performed. For batch sorption studies, PO_4 was measured by the standard ascorbic acid method (AAM). For transport studies, AsO_4 interference using the AAM necessitated the use of IC (Dionex AS4A-SC column) for PO_4 analysis.

3.2.2. Kinetic Adsorption Study

Separate batch studies were performed to evaluate the adsorption kinetics of AsO_4 and PO_4 onto the sand, and to determine an equilibrium time required for batch adsorption isotherm experiments. The batch kinetic adsorption experiments were performed in 15-mL polyethylene screw top bottles (Nalgene), and consisted of a 1:1 solid to solution ratio (5 g solid:5 mL solution), using initial concentrations of 150 μM AsO_4 and 360 μM PO_4. All solutions were prepared in a background of 0.01M KCl. Samples were collected at time intervals of 2, 4, 8, 24, 48, 96, and 168 h, and were decanted and filtered through 0.45μ nylon filters prior to analysis (AsO_4 by AA-HG, PO_4 by AAM). Adsorbed concentrations were determined by difference between initial and final measured solute concentrations. Approximately 97% of the equilibrium adsorbed AsO_4 concentration was reached within 24 h. The PO_4 adsorption had only reached 92% of the equilibrium concentration within 24h. Equilibrium (as defined by constancy of the ratio of adsorbed concentration to the concentration in solution) in both cases was not reached until at least 96 h.

3.2.3. Batch Isotherms

Batch adsorption isotherms for AsO_4 onto the sand were performed at three initial PO_4 concentrations (0 μM, 134 μM, and 1340 μM) in 35-mL polypropylene centrifuge tubes (Nalgene), using a 1:1 solid to solution ratio (15 g solid:15 mL solution). Initial concentrations of approximately 0, 1.3, 6.7, 13, 67, 133, and 266 μM AsO_4 were used at each initial PO_4 concentration. Samples were shaken for 96 h, and subsequently decanted and filtered through 0.45μ nylon filters prior to analysis for AsO_4 by AA-HG. Analysis of selected samples using IC indicated that, within the limits of detection, all of the total soluble As was present as AsO_4 species (i.e. As(V)). Adsorbed concentrations for AsO_4 were determined by difference between initial and final measured solute concentrations. Adsorption isotherms at each initial PO_4 concentration were fit to the Langmuir model using nonlinear regression according to the equation:

$$S=\Gamma_0 \frac{K_L \cdot C}{1+K_L \cdot C}$$

where S is adsorbed concentration (μmol kg^{-1}), C is solution concentration (μmol L^{-1}), K_L is an empirical affinity parameter (L μmol^{-1}), and Γ_0 is maximum adsorption density (μmol kg^{-1}).

3.2.4. Column Transport Experiments

Column transport experiments were performed on the sand under saturated conditions at three different pH values (4.5, 6.5, and 8.5) for a single AsO_4 concentration (133 μM) in conjunction with four different PO_4 concentrations representing molar P:As

ratios of 0, 0.1, 1.0, and 10. Column transport experiments were performed using 2.8-cm diameter, 8-cm length polycarbonate columns containing 76.5 g sand, resulting in a bulk density of ~1.55 g cm^{-3} and a calculated porosity of ~0.41. The end caps of the column consisted of fine nylon mesh (< 0.1 mm) supported by a Teflon plate drilled with 1-mm holes on 3-mm centers. A syringe pump (Soil Measurement Systems, Tucson, AZ) was used to provide flow to the columns.

Typical transport experiments were performed as follows. After initial saturation and conditioning with 0.01M KCl to the desired pH, approximately 1 pore volume of a tritiated water solution (^3H_2O in 0.01M KCl background, ~500 Bq mL^{-1}) was pulsed through the columns (direction of flow = bottom to top) at an average pore water velocity of 1 cm h^{-1} (0.25 mL pump volumes at a frequency of 350 s), followed by 0.01 M KCl. After complete recovery of the ^3H_2O pulse (~6 pore volumes total flow), one pore volume of a combined AsO_4/PO_4 solution was applied, followed by 0.01 M KCl. Four separate runs were performed at each pH value, keeping the AsO_4 concentration constant (133 μM; ~1650 Bq mL^{-1} ^{73}As), and varying the concentration of PO_4 (0, 13.4, 134, and 1340 μM). All pulse solutions were prepared in a background of 0.01M KCl. The experiments were continued until the tailing of AsO_4 in columns effluent was well established (~20 pore volumes) and AsO_4 concentrations were near baseline levels.

The native pH of column effluent was approximately 4.5. Application of numerous pore volumes of unbuffered 0.01 M KCl solutions at higher pH values (6.5 and 8.5) did not significantly alter the pH of column effluent. In addition, column effluent exhibited substantial pH change upon exposure to atmospheric CO_2. Consequently, a

carbonate buffered eluant solution of 0.01 M KCl was used to obtain constant column effluent pH values of 6.5 and 8.5. The buffered 0.01M KCl solutions were prepared by pH adjustment with KOH under conditions of continuous sparging with air until the pH of the eluant solutions had stabilized.

A separate column experiment was performed at pH=8.5 using degassed eluant solutions (sparged with N_2) to determine if the HCO_3^-/CO_3^{2-} concentrations in the $CO_2(g)$ buffered pH 8.5 systems significantly affected the transport of AsO_4 via HCO_3^- or CO_3^{2-} competition. Effluent pH values were measured with an in-line pH electrode to prevent sample exposure to atmospheric CO_2 prior to pH measurement. The experimental protocol was identical to the previous columns, and used the same AsO_4 concentration (133 μM; ~1650 Bq mL^{-1} ^{73}As) in the absence of PO_4.

An additional column experiment was performed to assess the effect of PO_4 on AsO_4 desorption in a column already loaded with an AsO_4 pulse. The column was conditioned (0.01 M KCl) and loaded with a 1 pore volume pulse of 143 μM AsO_4 (~1650 Bq mL^{-1} ^{73}As) at a pH of 4.5. After 20 pore volumes, the 0.01 M KCl eluant was replaced with an eluant containing 1420 μM PO_4 (10:1 molar ratio of P:As) in 0.01 M KCl. The experiment was continued for an additional 15 pore volumes until sufficient As tailing had been established.

A comparison transport study was performed using a column packed with an acid purified quartz sand (Fluka) at unaltered pH (~7.0). The column was conditioned with 0.01 M KCl, and loaded with a 1 pore volume pulse of a 133 μM AsO_4 solution and eluted according to the methods discussed previously. The experiment was continued

until sufficient tailing had been establish (~10 pore volumes), although AsO_4 recovery of > 95% was observed in column effluent within 5 pore volumes.

All column effluent was passed through an in-line 0.45μ nylon filter, and collected in glass test tubes using a fraction collector (~ 8 samples per pore volume). Effluent samples were analyzed for pH, followed by $^{73}AsO_4$ using liquid scintillation. Ion chromatography was used to analyze PO_4 concentrations and to verify that no reduction of arsenate to arsenite had occurred during transport. After termination, the sand from the columns was extracted with a mixture of 6N HCl and 3N HNO_3 to desorb the remaining adsorbed AsO_4, and the resulting extract analyzed for ^{73}As using liquid scintillation to determine mass balance of applied $^{73}AsO_4$. In all cases, the total recovery of applied $^{73}AsO_4$ was greater than 95%.

3.2.5. Determination of Column Transport Parameters

Individual sample volumes from the transport experiments were determined by the mass of the collected samples, assuming a specific density of 1 g-cm^{-3}, and water flux was determined as the average value of sample volume divided by the collection interval. Pore water velocity was then determined as the water flux divided by volumetric water content (θ_V), as determined by the equation $\theta_V = 1-(\rho_B/2.65)$ assuming a particle density of 2.65 g cm^{-3} and complete saturation in the columns, where ρ_B is the bulk density of the columns (g cm^{-3}). Relative concentration was determined as the ratio of the collected ^3H_2O or AsO_4 concentration to the applied ^3H_2O or AsO_4 concentration in the pulse, and the number of pore volumes was determined as the ratio of cumulative collected volume to

the liquid volume of a saturated column. Breakthrough curves (BTCs) for ^3H_2O were fit to the one-dimensional convection dispersion equation, with the computer program CXTFIT (Parker and van Genuchten, 1984), and were used to verify that no transport related nonequilibrium existed in any of the column runs. Dimensionless BTCs for AsO_4 were plotted using relative concentration vs. pore volumes ($V_{cumulative}/V_{Pores}$) of the column outflow. Cumulative recovery of applied AsO_4 collected in the effluent is also presented on all BTCs.

3.3. Results and Discussion

3.3.1. Batch Adsorption

The kinetics of AsO_4 and PO_4 adsorption onto the representative sand showed that at least 96 h was needed to reach equilibrium for both AsO_4 and PO_4 adsorption in a well mixed batch system (Figure 8). This is consistent with results from other studies showing a slow approach to equilibrium for AsO_4 adsorption onto amorphous Al hydroxides (Anderson et al., 1976) and ferrihydrite (Fuller et al., 1993). Similarly, PO_4 adsorption onto Fe and Al hydroxides has been shown to exhibit a slow approach to equilibrium (Bolan et al., 1985). The actual chemical step in the adsorption process of AsO_4 and PO_4 onto Fe and Al oxides and clay minerals is quite rapid, generally on the order of milliseconds (Grossl, 1995; Amacher, 1991; Sparks and Zhang, 1991). The slower approach to equilibrium observed in this experiment suggests that the kinetics of AsO_4 and PO_4 adsorption onto the sand were limited by mass transfer, such as film, intraparticle, and/or interparticle diffusion.

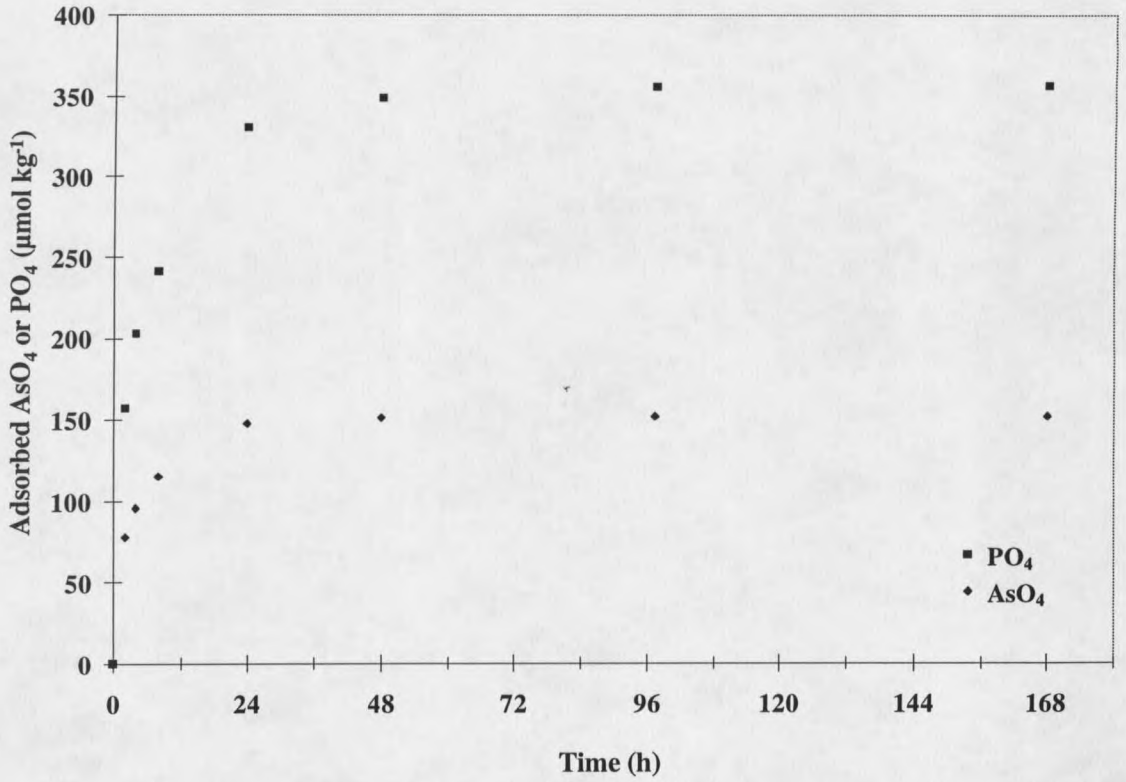


Figure 8: Adsorption kinetics of AsO_4 and PO_4 onto sand (single ion experiment) at a 1:1 solid:solution ratio (5 g (dry weight) solid:5 mL solution and at pH values ranging from 4 to 5 (AsO_4) and 4 to 5.7 (PO_4)). Initial concentrations were 150 µM AsO_4 and 360 µM PO_4 in a background solution of 0.01 M KCl.

Adsorption isotherms for AsO_4 onto the sand in the absence and presence of PO_4 show distinct Langmuirian behavior (Figure 9). The observed data were modeled by best fit Langmuir isotherms (nonlinear regression), yielding maximum site densities (Γ_0's) for AsO_4 onto the sand of 168, 112, and 7 µmol kg^{-1} in the presence of 0, 134, and 1340 µM initial PO_4 (0, 1:1, 10:1 molar ratios), respectively. The influence of PO_4 competition on AsO_4 adsorption by the sand (Figure 9) is consistent with AsO_4/PO_4 competition reported in other studies (Hingston et al., 1971; Goldberg, 1986). The presence of a 1:1 molar ratio of P:As resulted in a decrease of the maximum adsorption density of more than

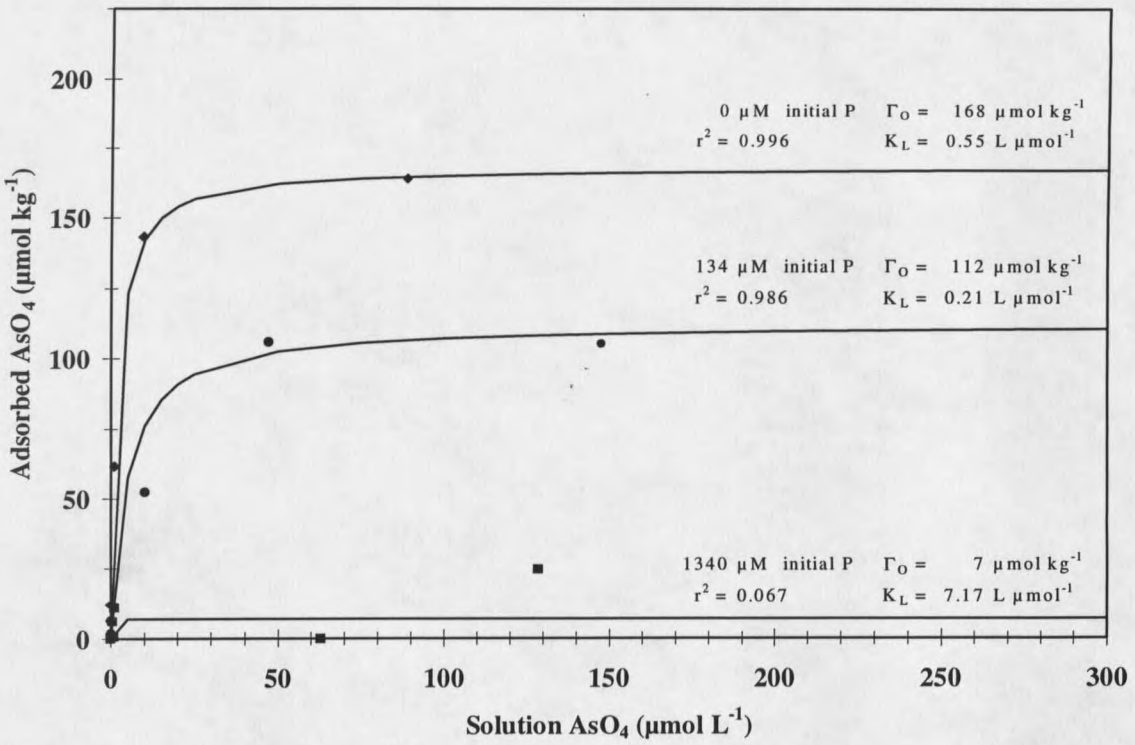


Figure 9: Adsorption isotherms (0.01 M KCl) for AsO_4 in the absence and presence of 134 µM and 1340 µM PO_4 at a 1:1 solid:solution ratio (15 g (dry weight) solid:15 mL solution) and a pH range of 4.0 to 4.6. Solid lines represent best fit Langmuir isotherms, where Γ_0 = maximum adsorption density and K_L = empirical affinity parameter.

33%. In the presence of a 10:1 molar P:As ratio, maximum AsO_4 adsorption was reduced by more than 95%.

Previous studies on the adsorption of AsO_4 by Fe hydroxides have shown that the maximum adsorption density of AsO_4 onto ferrihydrite is an order of magnitude greater than onto goethite (Pierce and Moore, 1982; Grossl, 1995, Hingston et al., 1971). At a pH of 6, Pierce and Moore (1982) reported a maximum site density for ferrihydrite of 0.12 mole AsO_4/mole Fe, although no surface area was reported for the ferrihydrite samples

used. At the same pH, Grossl (1995) reported a maximum site density for goethite of 0.0084 mole AsO_4/mole Fe with a sample surface area of 50 m^2/g, while Hingston et al. (1971) reported a maximum site density for goethite of 0.012 mole AsO_4/mole Fe with a sample surface area of 60 m^2/g.

Results of the citrate-dithionite (C-D) extraction indicate that the sand used in the current study contained about 0.01% by weight "free" iron oxides (Table 1). If it is assumed that all AsO_4 adsorption by the sand was a result of coordination with "free" iron oxide sites, a reasonable assumption given the strong preference of Fe oxide for AsO_4 compared to other soil phases (Fordam and Norrish, 1979; Jacobs et al. 1970; Johnston and Barnard, 1979; Livesey and Huang, 1981), then the maximum site density at a pH of 4.5 for the sand used in the current study was 0.095 mole AsO_4/mole "Free"-Fe. Pierce and Moore (1982) reported site densities on ferrihydrite of 0.16 and 0.12 mole AsO_4/mole Fe at pH values of 4 and 5, respectively, which is slightly greater than the calculated values for this experiment. However, Pierce and Moore (1982), used a batch-produced ferrihydrite in a well mixed system, which would likely have a higher surface area than the "free"-iron oxides present on the sand grains used in the current study

3.3.2. Effects of pH on As Transport

Breakthrough curves (BTCs) showing the effect of pH on the transport of AsO_4 through the sand are presented in Figure 10. The transport of AsO_4 at pH values of 4.5 and 6.5 exhibited significant retardation, tailing and poor recovery of applied AsO_4 (Figure 10). In contrast, the transport of AsO_4 at pH 8.5 was more rapid and resulted in a more

symmetrical BTC (Figure 10). After 10 pore volumes, the percent of applied AsO_4 recovered in the column effluent was 35.6, 39.2, and 100 for the columns at pH 4.5, 6.5, and 8.5, respectively. None of the predominant mineral phases present in the sand (quartz, feldspars e.g. Table 1) would be expected to sorb appreciable quantities of AsO_4. For comparison, the transport of AsO_4 through pure silica sand at pH 7 exhibited essentially no retardation or tailing with AsO_4 recovery in column effluent exceeding 95% within 5 pore volumes (Figure 11), which is consistent with the minimal adsorption of AsO_4 onto quartz observed in batch studies (Xu et al., 1991). It is thought that small quantities of

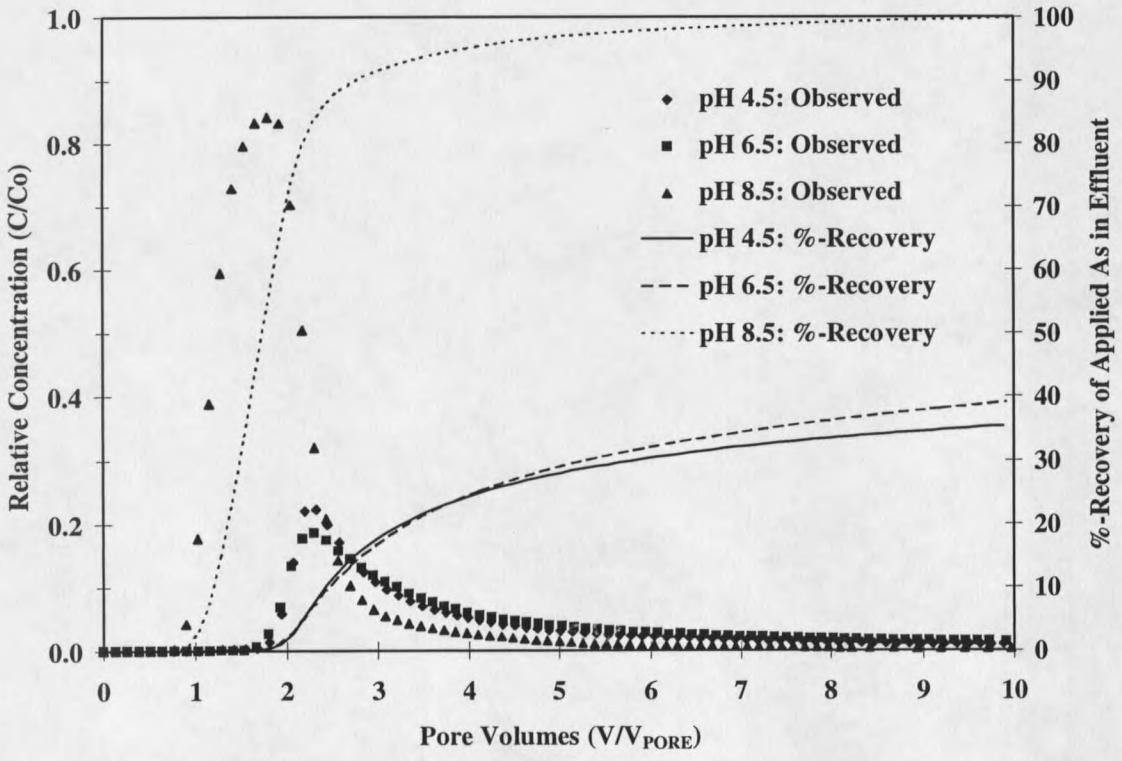


Figure 10: The transport of AsO_4 through a sand at three different carbonate buffered pH values: 4.5, 6.5 and 8.5 (Column conditions: Pore water velocity = 1 cm h^{-1}; Background = 0.01 M KCl; AsO_4 pulse = 1 pore volume at 133 µM).

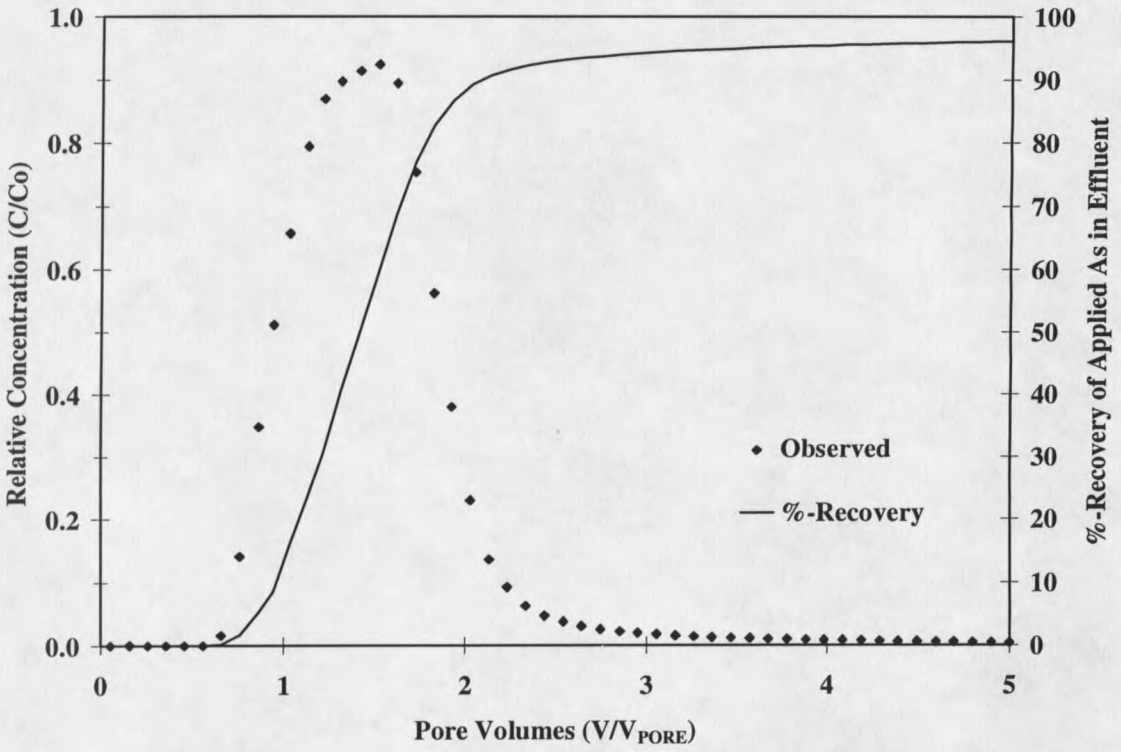


Figure 11: The transport of AsO_4 through clean quartz sand (Fluka) at pH 7 (Column conditions: Pore water velocity = 1 cm h^{-1}; Background = 0.01 M KCl; AsO_4 pulse = 1 pore volume at 133 μM).

"free"-Fe oxide present in the representative sand were responsible for the retardation and slow desorption of AsO_4 during transport at pH 4.5 and 6.5.

The enhanced transport of AsO_4 at pH 8.5 is consistent with surface complexation models describing the adsorption of AsO_4 by metal oxide surfaces, where sorption of AsO_4 decreases dramatically at pH values greater than 7 (Xu et al., 1991; Anderson et al., 1976; Pierce and Moore, 1982). Arsenate adsorption by Fe hydroxides can be categorized as a ligand exchange mechanism, and it has been shown by Extended X-ray Absorption Fine Structure Spectroscopy (EXAFS) that AsO_4 forms a combination of mono- and

bidentate complexes with surface Fe sites (Waychunas et al., 1993). For AsO_4 adsorption onto goethite, these ligand exchange reactions have been represented by (Goldberg, 1986; Grossl, 1995):

$$FeOH(s) + H_3AsO_4(aq) = FeH_2AsO_4(s) + H_2O$$
$$FeOH(s) + H_3AsO_4(aq) = FeHAsO_4^-(s) + H_2O + H^+(aq)$$
$$FeOH(s) + H_3AsO_4(aq) = FeAsO_4^{2-}(s) + H_2O + 2H^+(aq)$$
$$2FeOH(s) + H_3AsO_4(aq) = Fe_2HAsO_4(s) + 2H_2O$$
$$2FeOH(s) + H_3AsO_4(aq) = Fe_2AsO_4^-(s) + 2H_2O + H^+(aq)$$

and have been successfully described using the Constant Capacitance model. The pH dependence of AsO_4 sorption predicted from these reactions as described by Goldberg (1986) and Grossl (1995) supports the observation of enhanced transport at pH 8.5 observed in this study.

The sorption and subsequent transport behavior of AsO_4 as a function of pH is dependent both on the surface charge of the sorptive phase and on the aqueous speciation of AsO_4. Zero points of charge (pH_{ZPC}) for amorphous $Fe(OH)_3$ (ferrihydrite) and α-FeOOH (goethite) range from 8.5 to 7.8 (Stumm and Morgan, 1981). It is expected that the pH_{ZPC} for the "free"-iron oxide present in the sand would fall in this range; consequently we would expect that Fe oxide surfaces were predominantly positively charged at pH values of 4.5 and 6.5 and predominantly negatively charged at a pH of 8.5. The predominant AsO_4 species at pH values of 4.5 and 6.5 is $H_2AsO_4^-$, and at a pH of 8.5, the predominant species is $HAsO_4^{2-}$ (Figure 12). Consequently, at a pH of 8.5 the combination of a predominantly negative surface and a more negative AsO_4 solution species results in a dramatic increase in the mobility of AsO_4 (Figure 10).

To test the effects of HCO_3^-/CO_3^{2-} ions (present in the $CO_2(g)$ buffered systems) on the transport of AsO_4 at pH 8.5, column experiments were performed in both $CO_2(g)$ buffered and unbuffered ($N_2(g)$) systems (Figure 13). Effluent samples from both systems were periodically analyzed for total alkalinity yielding average values for carbonate concentrations of 1.2 mmol L^{-1} and < 0.1 mmol L^{-1} in $CO_2(g)$ and $N_2(g)$ systems, respectively. A value of 1.2 mmol HCO_3^- L^{-1} is consistent with equilibrium of $CO_2(g)$=0.0003 atm at pH 8.5.

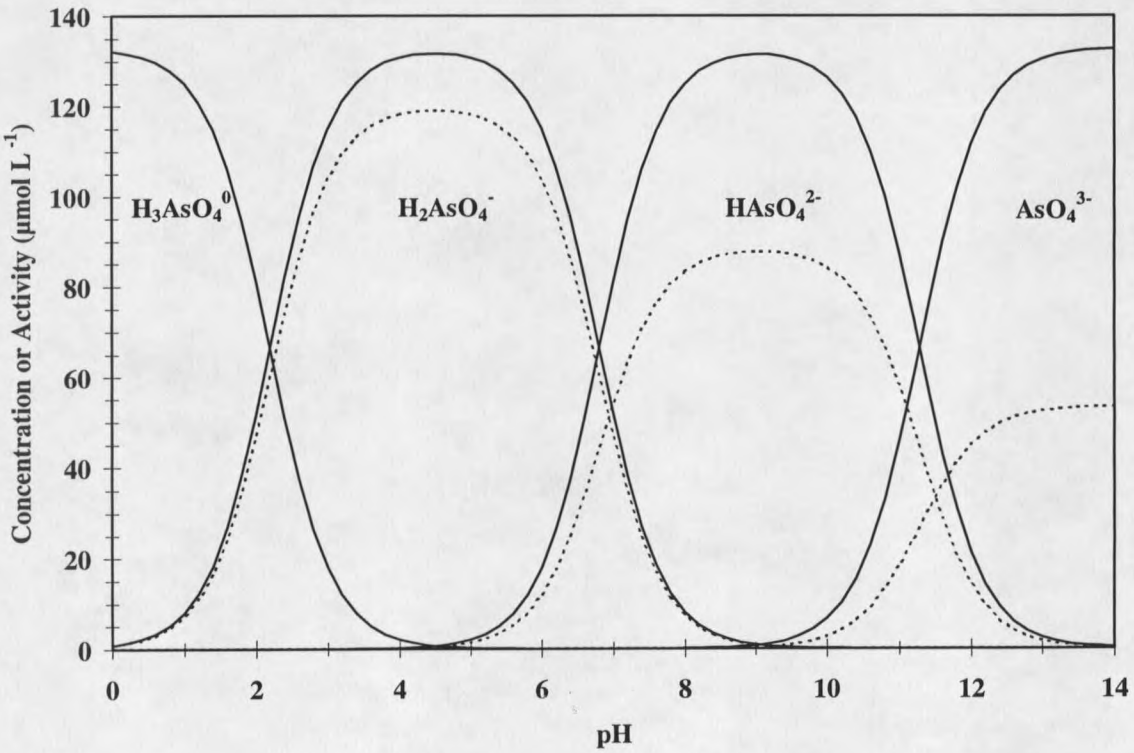


Figure 12: The distribution of AsO_4 species (solid lines represent concentration, dashed lines represent activity) as a function of pH for conditions specific to the column experiments (0.01 M KCl, 133 µM AsO_4); based on: pK_{a1}=2.24, pK_{a2}=6.94, pK_{a3}=11.5 (Sadiq et al., 1983).

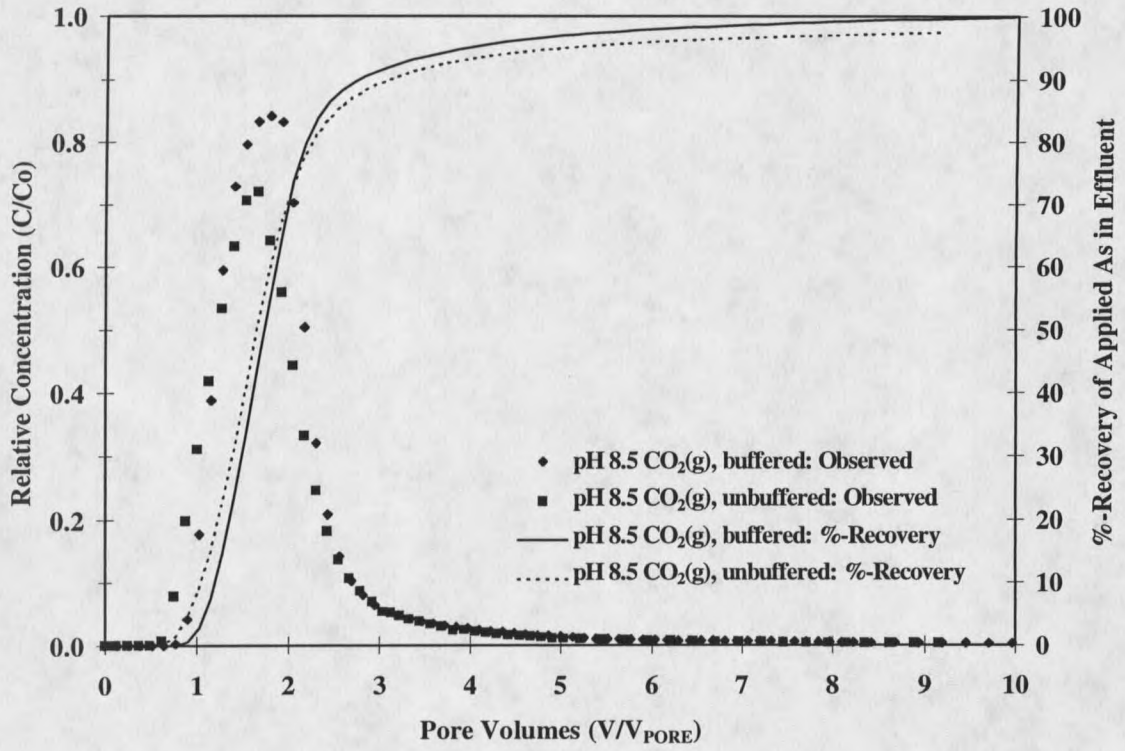


Figure 13: The transport of AsO_4 through sand at pH 8.5 in the presence and absence of CO_2(g) buffering (Column conditions: Pore water velocity = 1 cm h^{-1}; Background = 0.01 M KCl; AsO_4 pulse = 1 pore volume at 133 µM).

After 10 pore volumes of elution, the percent of applied AsO_4 recovered in the column effluent was 100% in the presence of CO_2(g), and greater than 95% in the N_2(g) system. While a majority (~ 90%) of the applied AsO_4 was eluted within 3 pore volumes, tailing was still observed in both columns (Figure 13). The transport of AsO_4 in the CO_2(g) buffered system exhibited a slight increase in recovery after three pore volumes, indicating that minor competition of HCO_3^-/CO_3^{2-} for adsorption sites may have occurred during transport. Results from this comparison confirm that enhanced transport of AsO_4 at pH 8.5 (Figure 10) was indeed a pH effect and not related to competition from HCO_3^-/CO_3^{2-} ions.

3.3.3. Effects of Phosphate Competition on As Transport

Breakthrough curves (BTCs) showing the effect of PO_4 competition on the transport of AsO_4 at pH 4.5 are presented in Figure 14. As the PO_4 concentration increased, recovery of the applied AsO_4 increased, and the AsO_4 BTCs were shifted to the left, indicating a decrease in retardation. After 10 pore volumes of elution, the percent of applied AsO_4 recovered in the column effluent was 35.6, 36.7, 63.5, and 88.4 for PO_4 concentrations of 0, 13.4, 134, and 1340 µM, respectively. With the addition of 1340 µM PO_4, the AsO_4 BTC occurred slightly after 1 pore volume, and had a peak concentration

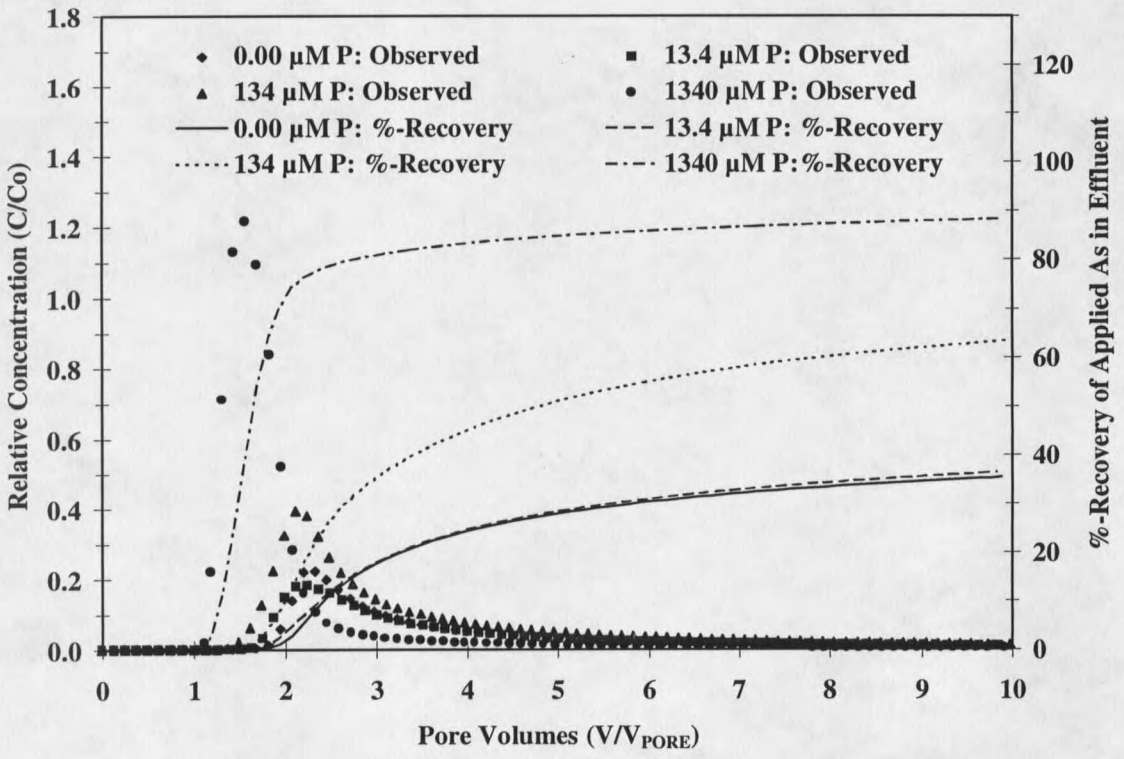


Figure 14: The transport of AsO_4 through sand at pH 4.5 in the presence of 0, 13.4, 134, and 1340 µM PO_4 (Column conditions: Pore water velocity = 1 cm h^{-1}; Background = 0.01 M KCl; AsO_4 pulse = 1 pore volume at 133 µM).

(C/C_0) near 1.2.

Breakthrough curves showing the effect of PO_4 competition on the transport of AsO_4 at pH 6.5 are presented in Figure 15. AsO_4 BTCs exhibited the same general behavior as the BTCs at pH 4.5, but in all cases the recovery of applied AsO_4 was greater at pH 6.5 than at pH 4.5, consistent with the effects of pH noted in Figure 10. After 10 pore volumes of elution, the percent of applied AsO_4 recovered in the column effluent was 39.2, 45.0, 67.9, and 91.6 for the columns at PO_4 concentrations of 0, 13.4, 134, and 1340

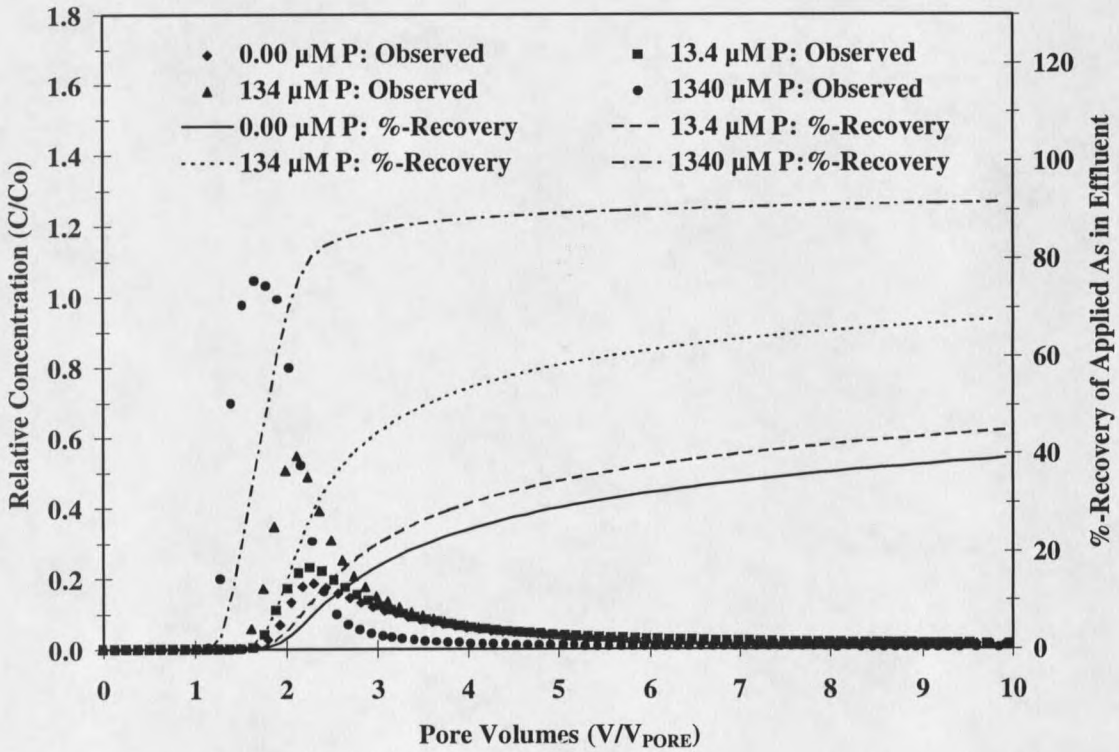


Figure 15: The transport of AsO_4 through sand at pH 6.5 (CO_2(g) buffered) in the presence of 0, 13.4, 134, and 1340 µM PO_4 (Column conditions: Pore water velocity = 1 cm h^{-1}; Background = 0.01 M KCl; AsO_4 pulse = 1 pore volume at 133 µM).

μM, respectively. Again, with the addition of 1340 μM PO_4, the AsO_4 BTC occurred slightly after 1 pore volume, and had a peak concentration (C/C_0) greater than 1.

Relative peak concentrations greater than 1 for AsO_4 BTCs at pH 4.5 and 6.5 in the presence of 1340 μM PO_4 indicate that AsO_4 was concentrated at the leading edge of the PO_4 BTC. Measurement of PO_4 concentration in the column effluent by IC verified that the PO_4 breakthrough occurred immediately after the AsO_4 BTCs. While recovery of applied AsO_4 was dramatically enhanced by the addition of 1340 μM PO_4 to the applied pulse, the recovery of applied AsO_4 still did not exceed 92%. This may indicate that certain sorption sites on the sand were specific for AsO_4, or that desorption kinetics of AsO_4 remain kinetically limited even in the presence of high concentrations of PO_4.

If it is assumed that all adsorption sites are equally available for either AsO_4 or PO_4, and are attributable to the "free" Fe-oxide sites on the sand, then the total adsorption capacity at pH 4.5 can be determined from the batch isotherm data as being 13.0 μmol (As or P) per packed column of sand. In a one pore volume pulse, the total input of AsO_4 was 2.7 μmol As, and the total input of PO_4 at molar P:As ratios of 0, 1:10 1:1 and 10:1 was 0, 0.27, 2.7, and 27 μmol P, respectively. Consequently. the resulting total column loading (AsO_4 plus PO_4) for column experiments was 2.7, 3.0, 5.4, and 29.7 μmol per pulse at molar P:As ratios of 0, 1:10 1:1 and 10:1, respectively. At a 10:1 molar P:As ratio, the total column adsorption capacity was exceeded by approximately 100%, indicating that there should have been sufficient PO_4 present in the column to compete for all adsorption sites.

An additional experiment was performed at pH 4.5 to evaluate the desorption of AsO_4 with a continuous pulse of PO_4 (Figure 16). After 20 pore volumes, recovery of a one pore volume pulse of 143 μM AsO_4 solution was only 20%. At 20 pore volumes, a 1420 μM PO_4 solution (10:1 P:As molar ratio with respect to the AsO_4 pulse) was applied as a continuous pulse. Arsenate recovery increased dramatically by more than 35% within 15 additional pore volumes of elution. The data indicate that the application of PO_4 onto an AsO_4 contaminated soil can result in a significant increase in pore water AsO_4 concentrations, consistent with other studies showing enhance mobility of AsO_4 in the

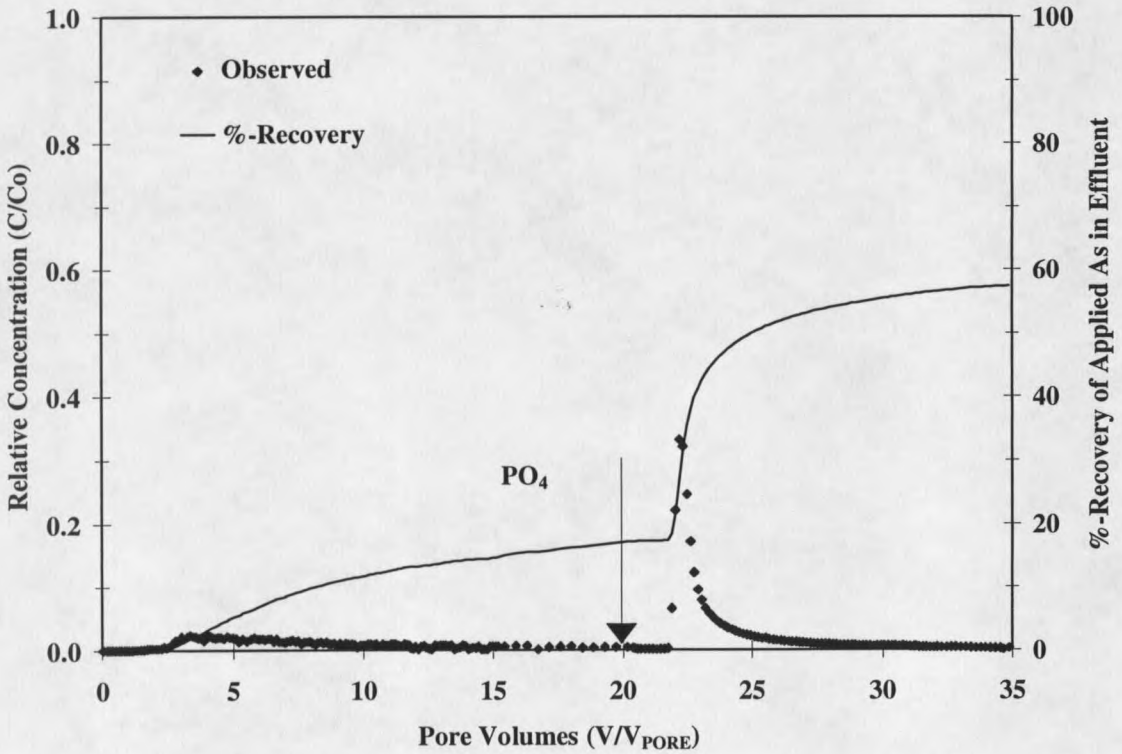


Figure 16: The transport of AsO_4 through sand at pH 4.5 followed by continuous addition of 1420 μM PO_4 at ~20 pore volumes (Column conditions: Pore water velocity = 1 cm h^{-1}; Background = 0.01 M KCl; AsO_4 pulse = 1 pore volume at 143 μM).

presence of PO_4 (Peryea 1991).

Significant AsO_4 tailing was observed after the first 5 pore volumes of PO_4 addition, indicating that a large fraction of the adsorbed AsO_4 was not readily desorbed by PO_4, even in the presence of excess PO_4. Furthermore, the percent recovery of applied AsO_4 in the effluent was still less than 60% after 15 pore volumes of PO_4 elution and 35 pore volumes total elution. It has been shown that transport of AsO_4 through the sand used in this experiment exhibits substantial kinetic limitations in both adsorption and desorption rates at pore water velocities ranging from 0.2 to 90 cm h^{-1} (Chapter 2). Consequently, it is possible that rates of AsO_4 desorption were slow with respect to pore water velocity, even in the presence of a strongly competing anion. Slow adsorption kinetics have been previously attributed to diffusion limitations within pore spaces of small aggregated particles in the case of PO_4 adsorption onto ferrihydrite (Willett et al., 1988). The sand used in the current study had a surface area (SA) of 0.39 m^2-g^{-1} (Table 1), which is more than 50 times the estimated geometric surface area (spherical). The higher SA indicates a large degree of surface roughness (Anbeek, 1992), suggesting that micropores existed on the sand particles. Finally, although no studies were performed in the current experiment to identify possible AsO_4 solid phase formation, our calculations of ion activity products (IAPs) suggest that our solutions were undersaturated with respect to AsO_4 solid phases. Furthermore, Waychunas et al. (1993) convincingly showed that scorodite formation on ferrihydrite was not important even at AsO_4 concentrations of 5 mM.

3.4. Conclusions

Arsenate was strongly sorbed to a sand, as determined by batch experiments and poor recovery of applied AsO_4 in the effluent of column transport experiments. The primary constituents present in the sand (feldspar, quartz) are not considered strong sorptive phases for AsO_4. The most likely reactive phase for AsO_4 sorption by the sand was Fe-oxyhydroxides as determined from selective dissolution of "free"-Fe oxides. At a pH above the expected pH_{ZPC} of the Fe-oxyhydroxide phase, AsO_4 transport through the aquifer sand increased dramatically, where AsO_4 recovery exceeded 95% within 10 pore volumes.

Phosphate was shown to effectively compete with AsO_4 for adsorption sites on the sand in batch isotherms as well as in saturated transport studies. This competition alone, however, was not sufficient to desorb all of the applied AsO_4 either in simultaneously applied pulses, or in a column where AsO_4 was applied prior to a concentrated PO_4 pulse. When the applied amount of PO_4 exceeded the calculated column adsorption capacity by two-fold, some AsO_4 remained adsorbed onto the sand. Likewise, when a high concentration of PO_4 (1420 μM) was continuously applied to a column that had been previously spiked with an AsO_4 pulse, recovery of AsO_4 in column effluent was still poor, even though the total PO_4 loading was greater than the calculated column capacity by more than two orders of magnitude. These results suggest that AsO_4 desorption kinetics were slow relative to the pore water velocity used in the experiments, and that desorption kinetics will play an important role in the transport of AsO_4 through porous media.

4. CONCLUSIONS AND GENERAL DISCUSSION

The current studies have resulted in several important considerations for predicting the transport of AsO_4 in contaminated soils and aquifers. Several specific conclusions can be reached as a result of this research:

(i) The use of batch derived equilibrium and kinetic partitioning parameters in the CDE failed to adequately predict the transport of AsO_4 under saturated conditions through what was considered to be a relatively nonreactive representative sand.

(ii) Curve fitting observed breakthrough data to the CDE using an nth-order kinetic sorption expression yielded different apparent rate coefficients at different pore water velocities, suggesting that the sorption rates are limited by diffusional processes. Such diffusionally limited processes are not taken into consideration in the basic CDE. Consequently, rate coefficients determined from well mixed batch systems or from any given column PWV cannot be readily extrapolated to all transport conditions.

(iii) pH was demonstrated to affect AsO_4 mobility in a manner that is consistent with results from previous batch studies and existing surface complexation models. It is likely that the controlling sorptive phase in our sand was amorphous Fe-oxyhydroxides. At a pH above the pH_{ZPC} for ferrihydrite (pH=8.5) recovery of applied AsO_4 exceeded 95% within 10 pore volumes

total flow, compared to a recovery of 35.6% at the native pH of the sand (pH=4.5).

(iv) Phosphate was shown to effectively compete with AsO_4 for sorption sites in the sand during transport, which is consistent with results from batch studies. However, PO_4 did not successfully compete for all sorption sites, even when present in extremely high concentrations suggesting the possibility of AsO_4 selective sorption sites or significant kinetic limitations in the desorption of AsO_4 from the sand.

(v) In the PO_4/AsO_4 competition studies performed at pH 6.5, an increase in the recovery of AsO_4 was evidenced (as compared with native pH = 4.5), which is consistent with lower sorption site densities predicted by surface complexation models.

(vi) Modification of pore water PO_4 concentration to a AsO_4 contaminated sand was shown to increase AsO_4 mobility, which is consistent with prior studies. However, even when total PO_4 loading exceeded predicted column capacity by more than two orders of magnitude, substantial amounts of AsO_4 remained adsorbed to the sand, suggesting that AsO_4 desorption kinetics can be limiting under the flow conditions that existed in the columns (PWV=1 cm h^{-1}).

4.1. Implications for Modeling

Many predictive transport models use the local equilibrium assumption (LEA) to describe sorption transport models in soil or aquifer systems, and the use of the LEA helps to greatly simplify the solution of the CDE. In instances where mass transfer or sorption kinetic limitations may exist, however, the LEA may be invalid. Consequently, it is important to understand the types of rate related processes and the relative magnitude of these processes that may be occurring in a natural system before applying the LEA in an attempt to predict contaminant transport. This study (Chapter 2) has demonstrated that in systems where small amounts of "free"-Fe oxides are the controlling sorptive phase in the soil, the LEA may not be applicable in describing AsO_4 transport at pore water velocities of 0.2 cm h^{-1} or greater.

Incorporation of a simple kinetic sorption expression into the CDE failed to account for the sorption partitioning that occurs during AsO_4 transport. The actual sorption process likely involves several steps, including bulk fluid diffusion, film diffusion, pore diffusion, particle diffusion, and finally the chemical sorption step. Any simple kinetic sorption model (e.g., nth-order) necessarily combines the effects of all of these processes into a single kinetic rate for the "sorption step". Furthermore, it is assumed that the modeled "sorption step" is dependent only upon resident solution and sorbed concentrations. Consequently, any diffusional dependence of the sorption processes on pore water velocity is lost in the use of a simple kinetic sorption expression.

The effect of pore water velocity on apparent kinetic sorption rate coefficients for the nth-order kinetic model was exhibited as an increase in apparent sorption rate and a

decrease in n value with increasing PWV. The apparently consistent trend would suggest that it might be possible to interpolate sorption rate coefficients within the range of pore water velocities studied in the column experiments. However, column studies were performed using a relatively homogenous disturbed sand that had been sieved so as to represent a uniform size fraction. Moreover, flow through the system was relatively uniform, very well characterized, and verifiable with the use of nonreactive tracers. The relative effects of diffusional processes occurring in the porous media can be expected to be strongly dependent upon physical structure of the porous media and extremely sensitive to disturbances. It is unclear the extent to which results from disturbed uniformly packed column experiments might be extrapolated to undisturbed porous media systems. Moreover, the relative magnitude of these diffusional processes to the chemical sorption step that occurs would be extremely site specific, and would require characterization of the porous media with respect to *in situ* pore water velocity distributions, surface and internal characteristics of the porous media, and reactive solid phases present. Consequently, extrapolation of independently (column) derived kinetic parameters for the nth-order kinetic sorption model to field scale predictions of AsO_4 transport would be of dubious value.

Previous models have been presented that incorporate diffusional processes that may occur during transport into the CDE (e.g., Nicoud and Schweich, 1989; Bahr and Rubin, 1987; Grove and Stollenwerk, 1985), and these models may provide improved description of As transport; however, there have been few studies directed towards experimental validation of such models. Grove and Stollenwerk (1985) presented both a

kinetic sorption model (Langmuirian) in the absence of diffusional processes, and an equilibrium sorption model in combination with film, pore, and particle diffusion to describe hexavalent chromium (CrO_4) partitioning during transport. Langmuirian sorption kinetics were described by (Grove and Stollenwerk, 1985; Rubin, 1983):

$$\frac{\delta s}{\delta t} = k_r' \left[c(\Gamma_0 - s) - \frac{1}{K_L} s \right]$$

where k_r' [$L^3 M^{-1} T^{-1}$] is a transformed reverse reaction rate (k_r/ρ), K_L is defined as the ratio of transformed forward reaction rate to transformed reverse reaction rate ($\frac{\rho}{\theta}\frac{k_f}{k_r}$), and other terms are the same as for the equilibrium Langmuir sorption isotherm (e.g., Section 3.2.3).

In the case where diffusional processes were considered to be controlling, Grove and Stollenwerk (1985) assumed that the chemical sorption step was instantaneous (equilibrium chemical sorption), and that the rate limiting step in the overall sorption reaction was either film-, pore-, or particle-diffusion. Diffusion-controlled sorption was modeled as (Grove and Stollenwerk, 1985):

$$\text{film diffusion: } \frac{\delta s}{\delta t} = \frac{k_{film} a_p \theta}{\rho}(c - c_e)$$

$$\text{pore or particle diffusion: } \frac{\delta s}{\delta t} = k_p a_p (s_e - s)$$

where k_{film} is the film mass-transfer coefficient ($L T^{-1}$), a_p is the external particle surface area per unit volume (L^{-1}), c_e is the solution concentration that would be in equilibrium with the sorbed concentration ($M L^{-3}$), k_p is the pore or particle mass-transfer coefficient

($L\ T^{-1}$), and s_e is the sorbed concentration that would be in equilibrium with the solution concentration ($M\ M^{-1}$).

Grove and Stollenwerk (1985) were able to achieve a reasonable description of CrO_4 transport in the absence of any diffusional processes using only a kinetically limited sorption model; however, the apparent sorption rate coefficients increased with increasing pore water velocity. Incorporation of a film diffusion term into the CDE (equilibrium sorption) provided improved description of CrO_4 transport as compared to the kinetic sorption model; however apparent film-diffusion rates were much less (1 to 2 orders of magnitude) than those predicted by empirical methods. The inclusion of pore or particle diffusion into the CDE (equilibrium sorption) provided increased description of CrO_4 transport as compared to the film diffusion model; however, apparent diffusional rate coefficients increased with increasing pore water velocity. The indication from the results of Grove and Stollenwerk (1985) is that no single process (chemical or diffusional) is significantly slow with respect to the other processes to be considered the sole rate-limiting step. Consequently, transport models may need to include a combination of more than one diffusional process (e.g., film- and pore-diffusion) and possibly kinetically limited chemical sorption to accurately describe contaminant transport under some flow regimes.

In summary, the use of a simple kinetic sorption model (nth-order) to describe AsO_4 partitioning during transport fails to account for PWV dependent diffusional processes that are significant during As transport. Furthermore, it appears as though such a model is not robust enough to be extrapolated to field scale predictions of AsO_4 transport in undisturbed systems. This research has pointed toward the necessity of

including descriptions of diffusional processes into As transport models. Existing models that consider the partitioning process to be limited solely by a single diffusional process (e.g., Grove and Stollenwerk, 1985) have the potential to improve description of As transport through porous media. It seems likely, though, that no single diffusional process may be limiting, and that incorporation of two or more diffusional steps into the CDE may be necessary to accurately describe As transport.

4.2. Implications for Soil Liming

Application of $Ca(OH)_2$ or CaO (soil liming) is a common management strategy for controlling metal mobility in contaminated sites such as mine tailings. The current study has indicated at pH values higher than the pH_{ZPC} of the controlling sorptive phase, transport of AsO_4 is accelerated in saturated, aerobic systems. Soil pH values after application of liming agents can exceed 10, which is much greater than the pH_{ZPC} for Fe oxide phases. Consequently, AsO_4 mobility can be expected to increase as a result of soil liming practices when Fe oxides are the controlling sorptive phase in the soil. This is consistent with recent work performed by Jones et al. (1996), which demonstrated that application of $Ca(OH)_2$ results in increased As mobility in some contaminated mine soils. The implication from this study is that traditional soil liming practices used to stablize metals in contaminated sites may not be particularly useful in stabilizing As, and may result in increased As mobility.

4.3. Implications for PO_4 Application

Equilibrium partitioning of AsO_4 and PO_4 between sorbed and solution phases can be determined with the use of competitive sorption coefficients (Hingston et al., 1971), or

by surface complexation models (Goldberg, 1986). However, it appears as though the use of equilibrium partitioning values determined by such approaches may grossly underestimate the desorption of AsO_4 from contaminated soils due to kinetic limitations that may exist during transport (Figure 16). This could have a substantial bearing on determination of the effects of PO_4 applications (e.g., fertilizers) to As contaminated soils.

The increase in AsO_4 mobility due to PO_4 competition evidenced in this study is consistent with prior published results AsO_4/PO_4 competition (e.g., Peryea, 1991; Roy et al., 1986a; Goldberg, 1986; Hingston et al., 1971). The previous work done on AsO_4/PO_4 competition, however, has typically been performed in well-mixed batch systems. The current study has demonstrated that substantial kinetic limitations can exist with respect to AsO_4 sorption processes during transport conditions in the presence of PO_4, and has evidenced the need for further understanding of these kinetic processes.

5. REFERENCES

Amacher, M.C. 1991. Methods of obtaining and analyzing kinetic data. In: D.L. Sparks and D.L. Suarez (eds.) Rates of soil chemical processes. Soil Science Society of America, Madison, Wisconsin. pp.19-59.

Anbeek, C. 1992. Surface roughness of minerals and implications for dissolution studies. Geochim. et Cosmochim. Acta. 56:1461-1469.

Anderson, M.A., J.A. Ferguson, and J. Gavis. 1976. Arsenate adsorption on amorphous aluminum hydroxide. J. of Colloid and Interfacial Sci. 54:391-399.

Bahr, J.M. and J. Rubin. 1987. Direct comparison of kinetic and local equilibrium formulations for solute transport affected by surface reactions. Water Resour. Res. 23: 438-452

Ball, W.P., M.N. Goltz, and P.V. Roberts. 1991. Comment on "Modelling the transport of solutes influenced by multiprocess nonequilibrium" by M.L. Brusseau, R.E. Jessup, and P.S.C. Rao. Water Resour. Res. 27:653-656.

Barrow, N.J. 1974. On the displacement of adsorbed anions from soils: 1. Displacement of phosphate by arsenate. Soil Sci. 116:423-431.

Bolan, N.S., N.J. Barrow, and A.M. Posner. 1985. Describing the effect of time on sorption of phosphate by iron and aluminum hydroxides. J. Soil Sci. 36:187-197.

Bouchard, D.C., A.L. Wood, M.L. Campbell, P. Nkedi-Kizza, and P.S.C. Rao. 1988. Sorption nonequilibrium during solute transport. J. Contam. Hydrol. 2:209-223.

Brusseau, M.L., T. Larsen, and T.H. Christensen. 1991. Rate-limited sorption and nonequilibrium transport of organic chemicals in low organic carbon aquifer materials. Water Resour. Res. 27:1137-1145.

Brusseau, M.L. 1992. Nonequilibrium transport of organic chemicals: the impact of pore water velocity. J. Contam. Hydrol. 9:353-368.

Brusseau, M.L. 1993. The influence of solute size, pore water velocity, and intraparticle porosity on solute dispersion and transport in soil. Water Resour. Res. 29:1071-1080

Cameron, D.A. and A. Klute. 1977. Convective-dispersive solute transport with a combined equilibrium and kinetic adsorption model. Water Resour. Res. 13:183-188.

Fordam, A.W., and K. Norrish. 1979. Arsenate-73 uptake by components of several acidic soils and its implications for phosphate retention. Aust. J. Soil Res. 17:307-316.

Frost, R.R., and R.A. Griffin. 1977. Effect of pH on adsorption of arsenic and selenium from landfill leachate by clay minerals. Soil Sci. Soc. Am. J. 41:53-57.

Fuller, C.C., J.A. Davis, and G.A. Waychunas. 1993. Surface chemistry of ferrihydrite: Part 2. Kinetics of arsenate adsorption and coprecipitation. Geochim. et Cosmochim. Acta. 57:2271-2282.

Gaber, H.M., S.D. Comfort, W.P. Inskeep, and H.A. El-Attar. 1992. A test of the local equilibrium assumption for adsorption and transport of picloram. Soil Sci. Soc. Am. J. 56:1392-1400.

Gaber, H.M., W.P. Inskeep, S.D. Comfort, and J.M. Wraith. 1995. Nonequilibrium transport of atrazine through large intact soil cores. Soil Sci. Soc. Am. J. 59:60.

Gamerdinger, A.P., A.T. Lemley, and R.J. Wagenet. 1991. Nonequilibrium sorption and degradation of three 2-chloro-s-triazine herbicides in soil water systems. J. Environ. Qual. 20:815-822.

Goldberg, S. 1986. Chemical modeling of arsenate adsorption on aluminum and iron oxide minerals. Soil Sci. Soc. Am. J. 50:1154-1157.

Goldberg, S. ad R.A. Glaubig. 1988. Anion sorption on a calcareous, montmorillonitic soil-arsenic. Soil Sci. Soc. Am. J. 52:1297-1300.

Grossl, P.R. 1995. Evaluation of contaminant ion adsorption/desorption on goethite using pressure-jump relaxation kinetics. Geoderma. 67:87.

Grove, D.B., and K.G. Stollenwerk. 1985. Modeling the rate-controlled sorption of hexavalent chromium. Water Resour. Res. 21:1703-1709.

Hingston, F.J., A.M. Posner, and J.P. Quirk. 1971. Competitive adsorption of negatively charged ligands on oxide surfaces. Discuss. Faraday Soc. 52:334-342.

Jacobs, L.W., J.K. Syers, and D.R. Keeney. 1970. Arsenic sorption by soils. Soil Sci. Soc. Am. J. 34:750-754.

Johnston, S.E., and W.M. Barnard. 1979. Comparative effectiveness of fourteen solutions for extracting arsenic from four western New York soils. Soil Sci. Soc. Am. J. 43:304-308.

Jones, C.A., W.P. Inskeep, and D. Neuman. 1996. Arsenic transport in contaminated mine tailings following liming. J. Environ. Qual. (to be submitted 1/96)

Lapidus, L., and N.R. Amundson. 1952. Mathematics of adsorption in beds. VI. The effect of longitudinal diffusion in ion exchange and chromatographic columns. J. Phys. Chem. 56:984-988.

Livesey, N.T., and P.M. Huang. 1981. Adsorption of arsenate by soils and its relation to selected chemical properties. Soil Sci. 131:88-94.

Nicoud, R.M., and D. Schweich. 1989. Solute transport in porous media with solid-liquid mass transfer limitations: Application to ion exchange. Water Resour. Res. 25:1071-1082.

Olson, R.V., and R. Ellis. 1982. Iron. *In* A.L. Page, R.H. Miller, and D.R. Keeney (eds.) Methods of soil analysis, Part 2. Agronomy. 9:301-312. Am. Soc. of Agron., Madison, Wis.

Parker, J.C., and M. Th. van Genuchten. 1984. Determining transport parameters from laboratory and field tracer experiments. Virginia Agricultural Experiment Station. Bull. No. 84-3.

Parker, J.C. and A.J. Valocchi. 1986. Constraints on the validity of equilibrium and first-order kinetic transport models in saturated soils. Water Resour. Res. 22:399-407.

Peryea, F.J. 1991. Phosphate-induced release of arsenic from soils contaminated with lead arsenate. Soil Sci. Soc. Am. J. 55:1301-1306.

Pierce, M.L. and C.B. Moore. 1982. Adsorption of arsenite and arsenate on amorphous iron hydroxide. Water Res. 16:1247-1253.

Roy, W.R., J.J. Hassett, and R.A. Griffin. 1986a. Competitive coefficients for the adsorption of arsenate, molybdate, and phosphate mixtures by soils. Soil Sci. Soc. Am. J. 50:1176-1182.

Roy, W.R., J.J. Hassett, and R.A. Griffin. 1986b. Competitive interactions of phosphate and molybdate on arsenate adsorption. Soil Sci. 142:203-210.

Rubin, J. 1983. Transport of reacting solutes in porous media: Relation between mathematical nature of problem formulation and chemical nature of reactions. Water Resour. Res. 19:1231-1242.

Sadiq, M., T.H. Zaidi, and A.A. Mian. 1983. Environmental behavior of arsenic in soils: theoretical. Water, Air, and Soil Poll. 20:369-377.

Selim, H.M., M.C. Amacher, and I.K. Isklandar. 1990. Modeling the transport of heavy metals in soils. U.S. Army Corps of Engineers, CRREL, Monograph 90-2.

Sidle, R.C., L.T. Kardos, and M. Th. van Genuchten. 1977. Heavy metals transport models in a sludge-treated soil. J. Environ. Qual. 6:438-443.

Sonderegger, J.L. and T. Ohguchi. 1988. Irrigation related arsenic contamination of a thin alluvial aquifer, Madison River Valley, Montana, U.S.A. Environ. Geol. Water Sci. 11:153-161.

Sparks, D.L., and P.M. Jardine. 1984. Comparison of kinetic equations to describe potassium-calcium exchange in pure and mixed systems. Soil Sci. 138:115-122.

Sparks, D.L. and P.C. Zhang. 1991. Relaxation methods for studying kinetics of soil chemical phenomena. In: Rates of soil chemical processes, Eds. D.L. Sparks and D.L. Suarez. Soil Science Society of America. pp.61-94.

Stumm, W and J.J. Morgan.. 1981. Aquatic chemistry: and introduction emphasizing chemical equilibria in natural waters. John Wiley and Sons, New York. p. 631.

Travis, C.C., and E.E. Etnier. 1981. A survey of sorption relationships for reactive solutes in soil. J. Environ. Qual. 10:8-17.

Valocchi, A.J. 1985. Validity of the local equilibrium assumption for modeling sorbing solute transport through homogenous soils. Water Resour. Res. 21:808-820.

van Genuchten, M. Th., J.M. Davidson, and P.J. Wierenga. 1974. An evaluation of kinetic and equilibrium equations for predicting of pesticide movement in porous media. Soil Sci. Soc. Am. J. 38:29-35.

Waychunas, G.A., B.A. Rea, C.C. Fuller, and J.A. Davis. 1993. Surface chemistry of ferrihydrite: Part 1. EXAFS studies of the geometry of coprecipitated and adsorbed arsenate. Geochim. et Cosmochim. Acta. 57:2251-2269.

Willett, I.R., C.J. Chartres, and T.T. Nguyen. 1988. Migration of phosphate into aggregated particles of ferrihydrite. J. Soil Sci. 39:275-282.

Xu, H., B. Allard, and A. Grimvall. 1991. Effects of acidification and natural organic materials on the mobility of arsenic in the environment. Water, Air, and Soil Poll. 57-58:269-278.

MONTANA STATE UNIVERSITY LIBRARIES
3 1762 10227787 6